



**Addis Ababa University**  
**School of Graduate Studies**

**THERMAL STRESSES AND CREEP  
ANALYSIS OF BOILER TUBES**

**By: Chanyalew Taye**

**Advisor: Dr. Alem Bazezew**

**Addis Ababa**  
**September 2004**



**Addis Ababa University**  
**School of Graduate Studies**

**THERMAL STRESSES AND CREEP**  
**ANALYSIS OF BOILER TUBES**

*A thesis submitted to the School of Graduate Studies of Addis Ababa University in partial fulfillment of the Degree of Masters of Science in Mechanical Engineering (Applied Mechanics stream)*

**By**  
**Chanyalew Taye**

**Advisor**  
**Dr. Alem Bazezew**

**Addis Ababa**  
**September 2004**

# Acknowledgment

During the course of my thesis work, there were many people who were instrumental and morally helping me. Without their guidance, help and patience, I would have never been able to accomplish the work of this thesis. I would like to take this opportunity to acknowledge some of them.

I would like to express my gratitude to my thesis advisor Dr. Alem Bazezew, whose expertise, understanding, and patience, added considerably to my graduate experience. I would like to thank all teaching staffs and my class colleagues in mechanical engineering department for the assistance they provided at all levels of the thesis work.

Special thanks go out to Dr. Ing. Demisse Alemu, without whose help and encouragement I would not have proceeded in graduate studies. He provided me with part time works at different areas which helped me to subsidize my tuition fees and accommodations. I doubt that I will ever be able to convey my appreciation fully, but I owe him my eternal gratitude.

I must give immense thanks to my sister Netsanet Alaye for her encouragement at all time in my life. I would also like to thank my friends Selam Girma and Askal Syoum for typing and editing the manuscript.

**Chanyalew Taye**  
**October 2004**  
**Addis Ababa**

# Table of Contents

	<b>Page</b>
<b>Acknowledgment</b> .....	<b>iii</b>
<b>Table of Contents</b> .....	<b>iv</b>
<b>List of Figures</b> .....	<b>vii</b>
<b>Abstract</b> .....	<b>viii</b>
<b>Chapter 1</b> .....	<b>1</b>
1. Introduction .....	1
1.1 Project Overview .....	1
1.2 Elevated Temperature Design Criteria .....	6
1.3 Objective of the Thesis .....	8
<b>Chapter 2</b> .....	<b>10</b>
2. Introduction .....	10
2.1 Literature Review .....	10
2.2 Organization of the Thesis .....	22
<b>Chapter 3</b> .....	<b>23</b>
3. Mathematical Modeling .....	23
3.1 Introduction .....	23
3.2 Stress Categories .....	25
3.3 Basic Theories and Assumptions .....	27
3.3.1 Theoretical background .....	27
3.3.2 Creep Curves at Constant Stress .....	28
3.3.3 Basic Assumptions .....	29

3.4	Derivation of Equilibrium Equation.....	30
3.4.1	Creep Strain.....	31
3.4.2	Cumulative Creep Laws.....	32
3.4.3	Elastic strain.....	36
3.4.4	Thermal Strains .....	40
3.4.5	Total strain .....	42
<b>Chapter 4</b>	<b>.....</b>	<b>43</b>
4	Solution Technique .....	43
4.1	Analytical Approach .....	43
4.2	Incremental Approach (Analytical).....	51
4.2.1	Governing Equations.....	52
4.2.2	Summary of Calculation Steps.....	56
4.3	Incremental Approach ( FEM ).....	57
4.3.1	Introduction .....	57
4.3.2	Method of Analysis .....	57
4.3.2.1	Derivation of Element Stiffness Relation .....	60
4.3.2.2	Multiaxial Stress-Strain-Time Relationships .....	62
4.3.2.3	Solution technique.....	63
4.3.3	Solution steps .....	64
<b>Chapter 5</b>	<b>.....</b>	<b>67</b>
5	Results and Discussion.....	67
5.1	Input description.....	67
5.2	Output Data and Discussion of Results.....	68

<b>Chapter 6.....</b>	<b>73</b>
6 Conclusion and Recommendation.....	73
6.1 Conclusion.....	73
6.2 Recommendation for Future Research.....	75
<b>References .....</b>	<b>77</b>
<b>Appendix A. ....</b>	<b>82</b>

# List of Figures

	Page
Fig. 3. 1 Creep curve obtained at constant temperature under constant load.....	29
Fig. 3. 2 Pressure loading and force equilibrium diagram .....	30
Fig. 3. 3 Time-hardening principle .....	33
Fig. 3. 4 Strain-hardening principle .....	35
Fig. 3. 5 Time-fraction principle .....	36
Fig. 3. 6 Cross-section of axisymmetric element.....	37
Fig. 4. 1 Simple cube element.....	43
Fig. 4. 2 Simplified creep curve at constant temperature under constant load .....	46
Fig. 4. 3 Infinite thick-wall tube discretized by triangular element.....	60
Fig. 4. 4 Triangular element.....	61
Fig. 4. 5 Program flowchart .....	66
Fig. 5. 1 Elastic stress distribution .....	70
Fig. 5. 2 Stress distribution due to temperature gradient .....	70
Fig. 5. 3 Effective total strain distribution .....	71
Fig. 5. 4 Effective total strain distribution (2D).....	71
Fig. 5. 5 Strain distribution at 10,000 hour .....	72
Fig. 5. 6 Elastic and relaxed stresses distribution .....	72

# Abstract

An analysis is developed for the calculation of creep deformation of an axisymmetric boiler tube subjected to axisymmetric load. The stresses and the permanent strains at a particular time and at the steady state condition, resulting from loading of the tube under constant internal pressure and elevated temperature were evaluated when accounts is taken to the secondary creep characteristics of a given material. In this thesis first the formulation of an analytical theory of creep for tubes according to the Bailey creep theory [41] was discussed. Bailey theory was proposed for an idealized homogeneous material loaded uniaxially. The theory takes into account the initial elastic strain, the transient creep strain, and the minimum creep rate strain. Next, more general solution by finite element method are presented and discussed for a class of problems in which no prior analytical solution may exists; like the cases of cracked and/or pitted boiler tubes. The method of solution is an extension of the direct stiffness method. The body is replaced by a system of discrete triangular cross-section ring elements interconnected along circumferential nodal circles. The equations of equilibrium for the body are derived from the principle of minimum potential energy. The creep behavior of the body is formulated in terms of creep laws in current use. Starting with the elastic solution of the problem, creep strains are treated as initial strains to determine the new stress distributions at the end of time interval. The procedure is repeated until either the final time is reached or until the stress distribution is not changed i.e. when a steady stated condition is reached. Calculated results according to arbitrarily selected boiler tube data are shown at the end.

## 1. Introduction

### 1.1 Project Overview

The object behind the successful operation of boiler is to take heat energy in its available form (for example, coal, oil, etc.) and to convert this heat energy into a form which can be conveniently used. This may be done by heating water in a boiler and then using the resulting hot water or steam for a desired purpose. There are many types of boilers developed in order to meet a variety of duties and ever-increasing output demands. Broadly boilers can be classified as: shell type (fire-tube), water tube and electric boilers.

Boiler tubes may fail in service condition due to many reasons. Some of these reasons are: *tube surface pitting, corrosion cracking, creep rupture, carbide graphitization, oxidation, sulfidation, embrittlement*, etc. These conditions which give rise to early failure of tubes are attributed to one or a combination of the following reasons [30, 47]<sup>\*</sup>:

- i.* the environmental conditions within the boiler can be highly aggressive and alter the microstructure of tubing.
- ii.* stresses caused by external loads, or induced by cold forming operations, uneven cooling or welding, may substantially lower the resistance of tubing to be attacked by certain corrosive media.

---

<sup>\*</sup> Show reference number

## **Pitting**

Pitting is a type of extremely localized attack which can be difficult to detect. Pitting is a destructive form of corrosion that affects the water side of boiler tubes. Surface imperfections and deposits can serve as initiation sites for pitting, and a consequent breakdown of the protective scale. The corrosive penetration depends on factors such as temperature, oxygen concentration, and lack of flow of fresh fluid to the pitted area.

## **Sulfidation**

Sulfidation or sulfide corrosion is a problem often encountered if there are reducing conditions in coal and oil fired boilers. Sulfidation can become a problem when temperatures exceed 260°C [30]. Sulfides may form scale on the tubing surface and cause damage, because the scale is easily changed to powder and subject to exfoliation; or the sulfides with their comparatively low melting point may fuse with the tubing surface and cause rapid inter-granular penetration.

## **Embrittlement**

During exposure at elevated temperatures between 400°C and 540°C, high-chromium ferritic and martensitic steels, as well as the ferrite phase in duplex austenitic-ferritic stainless steels are subject to a form of embrittlement [47]. This condition is known as 475°C embrittlement because maximum embrittlement occurs at this temperature. The condition is characterized by an increase in hardness and a loss in toughness. At chromium levels greater than 15% the embrittlement may be observed in long-time exposures at temperatures at least as low as 260°C, depending upon the chromium and alloy content. At

chromium levels of 13% or 14%, a modest increase in hardness may be seen in long-time exposure at 480°C [28].

### **Carbide graphitization**

The carbide phase of carbon and carbon-moly steels may be converted to graphite after long-time exposure to high temperature. If this occurs locally as sometimes associated with weldment, especially in headers and steam piping, structural integrity may be adversely affected. If it occurs, generally slight losses of strength and ductility can be expected. In carbon steels, such conversion to graphite may occur on prolonged exposure to temperatures exceeding about 425°C. In carbon-moly, the conversion may occur on prolonged service above about 470°C [28, 35].

### **Oxidation**

Resistance to oxidation is one of the most important characteristics of alloy and stainless grades. The chromium in these grades reacts with oxygen to form a tight, adherent scale that retards oxidation at elevated temperatures. As the chromium content increases, the degree of protection and the maximum operating temperature increases for the tubing.

### **Stress corrosion cracking**

Austenitic chromium-nickel steels that are highly stressed in tension may develop transcrystalline or intercrystalline cracks when simultaneously exposed to a specific aqueous corrosive medium. The austenitic stainless steels are very susceptible to chloride

stress corrosion cracking. Dissolved oxygen is essential to the cracking of the austenitic stainless steels in solutions containing chlorides or other halides.

### **Short-term Overheat**

Short-term overheat failures are most common during boiler start up. Failures result when the tube metal temperature is extremely elevated from a lack of cooling steam or water flow. A typical example is when superheater tubes have not cleared of condensation during boiler start-up, obstructing steam flow. Tube metal temperatures reach combustion gas temperatures of  $870^{\circ}C$  or greater which lead to tube failure. Failure results in a ductile rupture of the tube metal and is normally characterized by the classic “fish mouth” opening in the tube where the fracture surface is a thin edge.

### **Long-term Overheat (Creep)**

Long-term overheat occurs over a period of months or years. Superheater and reheat tubes commonly fail after many years of service, as a result of creep. During normal operation, alloy superheater tubes will experience increasing temperature and strain over the life of the tube until the creep life is expended. Furnace water wall tubes also can fail from long-term overheat. In the case of water wall tubes, the tube temperature increases abnormally, most commonly from waterside problems such as deposits, scale or restricted flow. In the case of either superheater or water wall tubes, eventual failure is by creep rupture.

Creep is a time-dependent deformation which occurs when a material is stressed at high temperature. Over a period of time with a continued load, the material will eventually

rupture. The temperature at which creep becomes important depends on the particular metal. For carbon steel, creep rupture becomes a design consideration at 425°C, for alloy steels at about 480°C and for austenitic stainless steels at about 560°C [41]. The failed tube has minimal swelling and a longitudinal split that is narrow when compared to short-term overheating. Tube metal often has heavy external scale build-up and secondary cracking.

Creep rupture can be avoided in tubing by selecting a grade of steel whose creep rupture strength is sufficient to withstand the specific operating conditions. For boilers creep and creep rupture data have been used as part of the criteria for establishing maximum allowable working pressures. The values are listed in *ASME Boiler and Pressure Vessel Code, "Section VIII, Power Boilers"* [32]. Designing and operating at the corresponding design conditions will prevent almost all failures of this type.

The phenomenon of creep rupture is one of formation of voids by sliding or shearing forces at grain boundaries, and the enlargement and coalescence of these under tensile forces. These voids concentrate primarily at grain boundaries normal to the maximum applied stress and final fracture is predominantly a brittle inter-granular one obeying the maximum principal stress theory of failure. Material damage accumulates with time with the result that the proportion of the material available to carry load is reduced, thereby increasing the applied stress until fracture occurs. This damage (voids, fissures, cracks, etc.) occurs essentially uniformly over a relatively large cross-sectional area, or volume, of the material and the resulting stress is an average one.

Almost all of the breweries, food complexes and textile factories in our country are equipped with different types of boilers. From experience we know that most of them have problems with the ruptured fire chamber or flue gas tubes. Though we have this common day to day problem, there is no any qualified organization engaged to undertake the corrective action of ruptured boiler tubes. In order to undertake appropriate corrective action for ruptured tubes subjected to combined loads, proper knowledge of the stress distribution along the tubes is important. Thus we think the study of thermal stresses and rupture analysis is a roadmap for a professional organization to be established for the proper maintenance of ruptured boiler tubes.

## **1.2 Elevated Temperature Design Criteria**

The time factor, which can be ignored at lower temperatures, is an essential ingredient of elevated temperature design criteria. Current rules (like the ASME boiler and pressure tube code) reflect the time-dependence of both materials properties and structural behavior. Component design life is explicitly considered, and the concept of life fraction summations is utilized in the basic load controlled stress limits. Strain limits, creep fatigue damage criteria, and creep ratcheting rules are also included.

Obviously, inelastic analysis methods should be a part of any satisfactory high-temperature design techniques. To adequately guard against failure resulting from time dependant inelastic behavior, without introducing extreme conservatism, the stress and deformation history must be predicted throughout the life of a structure.

## **Inelastic Analysis Methods**

Generally, unless otherwise justified, an elastic structural analysis for high-temperature conditions requires a combined time independent elastic-plastic analysis and time-dependant creep analysis in which creep and elastic plastic behavior are simultaneously considered.

### **Time-independent Elastic-plastic Behavior**

Three ingredients, in addition to Hooke's law are necessary to describe material behavior for an elastic plastic analysis [31]. These are:

1. yield criterion, specifying the states of multiracial stress for which plastic flow first sets in,
2. flow rule in the form of equations relating plastic strain increments to the stresses and stress increments subsequent to yielding; and
3. hardening rule, specifying the modification of the yield condition in the course of plastic flow.

### **Time-Dependant Creep Behavior**

Constitutive equations based on the equation of state require three ingredients, some what similar to the ingredients required to describe elastic-plastic behavior [41]. These are:

- i.* uniaxial creep equation describing the experimental, uniaxial, constant-stress, creep curves
- ii.* so called "flow rule" for generalizing the uniaxial equation to the multiaxial conditions; and

*iii.* hardening law for generalizing the constant stress creep law to variable conditions

The uniaxial creep equation can, theoretically, be any convenient algebraic equation that adequately describes the creep curves. The particular equation, or “creep law” used depends, of course, on the creep data for the material of interest. For the flow rule, the concepts of effective stress and effective creep strain are introduced, together with the following assumptions [31]:

- i.* creep deformations occur under constant volume
- ii.* the hydrostatic stress state does not influence creep deformations
- iii.* the principal direction of the stress and creep-strain-rate tensors coincide in an isotropic medium

### **1.3 Objective of the Thesis**

The specific objective of this thesis work is to demonstrate the thermal stress analysis and develop a code to be used to analyze creep behavior of boiler tubes. The objective includes in general terms the following.

- Derivation of general relationships for determining the limiting stresses in boiler tubes.
- Estimation of the life time of boiler crack free tubes under creeping mode.
- Making suggestions and recommendations in preventive maintenance procedures of boiler tubes and repair of ruptured tubes based on the creep life estimation.

These objectives will be achieved by employing the following procedures:

- Modeling of the tubes as an end constrained thick wall cylinder subjected to internal and external pressure at elevated temperature.
- Deriving governing equations to determine the radial and tangential stresses.
- Study the effects of flue gas temperature on clean tubes and tubes covered with scale or soot, and the effect while shortage of feed water inside the shell.
- Analysis of creep failure time of tubes in reference to operating pressure and temperature.
- Commenting on the analysis of creep in the presence of longitudinal or circumferential through-crack in the tube

## 2. Introduction

### 2.1 Literature Review

When metals are subjected to stress at temperatures in excess of  $0.33T_m$  where  $T_m$  is the absolute melting temperature, the metal suffers time-dependent creep deformations. In addition, internal damage increases with time and ultimately the metal ruptures. Therefore, when designing shell structures operating at such evaluated temperatures, consideration must be made to ensure that creep deformations do not exceed operational requirements during the life of the component. Common allowable strains are 1% average and 5% maximum [21].

During the last hundred years there was a large amount of published materials on creep mechanics mostly influenced by various approaches in establishing suitable constitutive equations. The relations were verified by the practical use of the proposed constitutive equations in structural analysis (thin-walled structures like tubes, discs, plates, shells, etc.). By establishing suitable constitutive equations, which give the strain rates and the rate of internal damage of the material, it is possible in principle to establish by numerical means the strain, stress and damage history at all points in the shell.

Design of parts for elevated temperatures where a condition of general creep will occur presents two principal requirements. A satisfactory means is necessary for determining the stress distribution and for relating creep in the practical case, which is usually one

involving compound stress, with that of simple tension for which practically all test data have been obtained. Also, it is necessary that test data be obtained under conditions comparable with those in practice, particularly in regard to the amount of creep permissible and any weakening effect of service upon the material.

Bailey [41] is the pioneer of presenting a useful work in the study of design aspect of creep, 1935. He proposed general expression for creep in terms of principal stresses based on simple tension test. He performed several experiments to verify the validity of those general creep expressions and got good agreement.

Satisfactory estimate of a correlation of tension creep test with relaxation tests was made by Popov [40], in his PhD dissertation work. The validity of methods for simple relaxation is demonstrated on the bases of experimental agreement between calculated and test results. The formulations for tension creep curves were established. Then the analytical schemes that appear satisfactory are extended for relaxation with the elastic follow-up.

The consideration of primary creep in the design of internal-pressure vessels was proposed by Coffin et al [38]. In their paper the evaluation of permanent strains and stresses at a particular time resulting from loading a thick-walled cylinder under constant internal pressure and elevated temperature when account is taken to the primary creep characteristics of a given material. The results are compared with permanent strains obtained by considering secondary creep as the general bases for pressure vessel design. Till then the commonly accepted bases for design of pressure vessel at elevated temperatures has been by the use of tensile secondary-creep data applied to combined

steady stress such as the method used by Bailey [41]. They show how the tensile primary-creep characteristics may be utilized in the design of thick-walled pressure vessels. In other words, they showed the stress-deformation history of the tube from the time when the pressure is applied initially until its life expectancy, or to the time when steady-state conditions corresponding to secondary creep are reached.

Yoh-han Pao and Marin [43] formulate an analytical theory of creep deformation of materials. The theory was proposed for idealized materials and may be applied to those materials whose behavior conforms to that idealized material. In the theory, the initial elastic strain, the transient creep strain, and the minimum rate creep strain are taken into account.

Creep analysis of axisymmetric bodies using finite elements for calculating the creep strains was developed by Greenbaum and Rubinstein [37]. The method involves starting with the elastic solution of the problem and calculating the creep strains for a small time increment. Those creep strains for a small time increment. Those creep strains are treated as initial strains to determine the new stress distribution at the end of the time increment.

Next we will outline some of the available literatures from 1975 to date as follows. Lower bounds on rupture times of thick-walled tube in pure torsion and a hollow sphere under constant internal pressure were obtained by Goel [2] and numerical values of rupture time for the tube case with different forms of damage rate laws were presented. The type of damage law assumed makes a significant effect on predicting the time to rupture but failure in all cases occurs almost instantaneously after the appearance of first crack.

A structural element in creep may rupture in any of the two modes of failure, namely, ductile and brittle. When a structural component is subjected to high stress levels failure may occur due to the geometric instability caused by necking; such a failure is called ductile failure. On the other hand, structures at low stresses and high temperatures may exhibit brittle failure. It happens due to the degradation of the microstructure of the material. Fissures and voids are usually found where such a failure occurs and these voids and fissures grow on planes which are perpendicular to the direction of the maximum principal stress.

Ponter [20] described creep constitutive relationships based on Bailey-Orowan theory. Displacement and work bounds are derived from the general theory for a body subjected to variable thermal and mechanical loading. Special cases are discussed, including isotropic-hardening plasticity and the bounds are related to certain elementary continuum problems. For cyclic loading the bounds relate to the exact solution when the cycle time is small compared with characteristic material times.

Cooks and Leckie also developed constitutive relations, based on the Baily-Orowan's creep theory [21-22]. They derived constitutive relations for "Deformation Bounds for Cyclically Loaded Shell Structures Operating under Creep Conditions" and "Creep Rupture of Shell Structures Subjected to Cyclic Loading". A bounding theorem on displacement is obtained for structures subjected to cyclic loading and application of the bound is illustrated.

The non-buckling finite deformations of an orthotropic thin wall cylinder are investigated by Orgill and Wilson [26] for a cylinder made of a nonlinear material and subjected to strains in the cylinder where were assumed to be axially homogeneous. The model is then extended to include axially non-homogeneous stresses and strains that may arise due to particular displacement boundary conditions such as radial confinement at the edges. The loads are applied to the cylinder incrementally, the finite strains are computed and adjustments are made in cylinder dimensions and the constitutive law to account for geometric and material nonlinearities.

Again within the framework of classical elasticity, the non-buckled deformations are calculated for orthotropic, right circular, thin-walled cylinders under uniform load conditions [19]. The principal direction of orthotropy follows parallel constant angle helices. Non-dimensional system parameters involving four material constants and three loading conditions (internal pressure, longitudinal load, and pure torque) are identified. Through parametric studies deformation patterns are calculated that are unique to orthography. Numerical examples illustrate that the proper selection of cylinder orthotropy can lead to designs with optimal deformations or load-carrying capacity which may be used for the design of robotic actuators driven by internal pressure.

Hyer and Cooper [25] have presented a linear elastic solution for determining the response of composite tubes subjected to a circumferential temperature gradient of the form  $\Delta T_o + \Delta T_1 \cos \theta$  which is assumed not to vary with distance along the tube nor through the wall. Previously, considerable work had been done to understand the response

of single and multiple layers of fiber-reinforced materials in tubular form to bending, torsion and tensile loads. In their work, they assumed temperature-independent material properties and used a displacement approach. The results are limited to tubes with the fibers in each layer oriented axially or circumferentially, so-called cross-ply tubes. Numerical results show that fiber orientation strongly influences the stresses in a single layer tube. When the fibers are aligned axially, all components of stress in the tube are small. When the fibers are aligned circumferentially, the hoop stress becomes large.

The temperature distribution and thermal stresses in asymmetrically heat radiated tubes were considered by Fett [18]. The transient and stationary temperature distributions in a tube wall caused by an asymmetrical heat flux distribution are evaluated. The results are represented for the case of a heat radiating half-space. In addition, the accompanying stress distributions are computed. In their work analytical solution of this problem was communicated.

Zarrabi et al have done substantial work in the area of boiler tube life analysis since 1990's. A simple method was developed to estimate the life of boiler tubes of fossil-fuel power plants by Zarrabi [16]. The method is applicable when the dominant mode of failure is creep rupture and/or plastic collapse followed by fracture in the presence of tube thickness loss caused by corrosion and/or erosion processes. The method uses both ISO and projection rupture data; and does not require creep stress index as an input.

Later around 1994 with the initiative of the University of new south Wales (UNSW) and in collaboration with the pacific power and Australian Nuclear and scientific Technology

organization (ANSTO), a research and development project has been formulated for life assessments of boiler tubes by Zarrabi and Zhang [13]. A  $P^*$  parameter is described that can be used to determine the primary stress in a scarred boiler tube. The scar may be due to localized erosion or corrosion. This primary stress can then be used as one of the ingredients for estimating the tube life. The project consists of two major systems, namely: an off-line system and an on-line system. Each system provides the tubing life using both deterministic and probabilistic models. Although there were a number of computer codes for estimating the life of boiler tubing, the off-line system that has been developed under the above-mentioned project is unique with respect to the following:

- normally the tube thinning is assumed to be uniform and extended along the entire tube. The off-line system allows for localized erosion, corrosion or tube scars.
- the existing computer programs were mainly applicable to super heater and re-heater tubing that operate within creep range. The offline system is
- applicable to economizer and water-wall tubing that operates below creep range as well as super heater and re-heater tubing.

To obtain the tubing life the three parameters that need to be known are: the tube geometry, material properties, and operational loads. Knowing the tube geometry and loading-conditions, the tube stress is calculated as a function of time. Combination of the tube stress with material properties at operating temperature will lead to tube life determination.

Erosion or corrosion causes the tube to become progressively thinner and as a result of which the primary stress in the tube increases with time. Extensive elastic-plastic finite

element analysis needs to be performed to obtain the primary stresses in the localized thinned section of a tube. That may be the basis for the first time to model localized thinning and scars in the boiler tubing. The thinned sections due to pitting were modeled as a groove on the surface of the tube. Therefore the stress and strain analysis was performed due to the stress concentration.

A robust (simple and conservative) method for determining the creep life of a defect-free component subjected to uniform load and temperature is also described by Zarrabi and Toudeshky [14]. This method has been specifically developed for the components containing stress concentrators. It is called the UNSW-LIFE2 method and requires only the elastic stresses, the uneasily creep rupture data and the steady-state creep solution for the plain component excluding stress concentrators where the latter is readily available from literature and is normally simple to calculate.

Another very important work of Zarrabi and his co-workers is the “Estimation of metal temperature variations for scarred boiler tubes, 1996” [15]. The paper describes the development of a non-dimensional parameter termed  $T^*$ . It is shown that  $T^*$  can be used to estimate the tube temperature variation in the scarred tube section. Also a method has been described for volume and characterization of a tube scar. This is important for more accurate tube life assessments. The plant engineer can predict the remaining life of boiler tubes installed in a fossil-fuelled power plant if the stress and average temperature history of the tubes are known, together with the way the tubing is thinned as a result of erosion and corrosion processes.

One of the powerful methods that are currently available for the design and life assessment of the components that operate within the creep range is the reference stress (RS) method. However, for problems for which the RS is not available from existing solutions, one usually needs to use a non-linear finite element method which is normally iterative, time-consuming and computationally expensive. An efficient and effective method for computing an approximate value for RS is described that combines a lower-bound theorem and finite element decartelization by Zarrabi and Motalagh [12]. The resulting quadratic programming is solved by an active set of finite element formulation algorithm. The verification and application of the proposed method are also described.

The stress algorithm for a non-linear kinematics hardening model is derived by Meggyes [17]. The algorithm is implemented in a FEM code and on a simple shear test; they compared the numerical results with the analytical ones.

The analysis of creep-damage processes is becoming more and more important in engineering practice due to the fact that the exploitation condition like temperature and pressure are increasing while the weight of the structure should decrease. In the same time the safety standards are increasing too. The accuracy of the mechanical state estimation (stresses, strains and displacements) mainly depends on the introduced constitutive equations and on the chosen structural analysis model. Altenbach in his work “A Non-classical Model for Creep-Damage Processes”, for the first purpose an improved generalized phenomenological creep model is introduced and extended to the case of creep-damage coupling. In addition, a micrometrical-based model is discussed. For thin-walled

structures under creep-damage conditions, the advantages and the problems of different approaches were discussed.

Continuum damage theory has proven to be an effective tool in creep damage simulation. In order to establish some mechanical principles for life extension of components at elevated temperatures, a numerical scheme based on the localized creep damage theory is introduced by Ling et al [23]. To illustrate the strength potential of structures for life extension, the method was first applied to a simple case of two-bar structure. Based on the considered simple case, typical components of geometrical discontinuity, material discontinuity, and temperature inhomogeneity were analyzed. In terms of the damage distribution or exhaustion of the components, some principles for life extension were proposed.

Nonlinear FEA of pressure vessels requires careful engineering judgment, experience and powerful analysis software. Sîanal [10] presents two pressure vessel problems, where the large displacement and plastic straining response of the structure is simulated by geometrically and materially nonlinear finite element analysis. The first application case involves the limit load prediction of imperfect tubes (with ovalized cross-sectional shape) under external pressure and discusses the accuracy of the pressure vessel code formula. The second case simulates the large-strain cold-deforming process of a pressure vessel made from a strain-hardening steel. In each case, special aspects and pitfalls of a nonlinear analysis have been discussed and some recommendations are given to the stress analyst.

In life assessment, the effect of a pre-existing stress field on the behavior of a crack at high temperatures needs to be addressed. Kwon et al [6] considered the effects of residual stresses in crack growth of cold bent and longitudinally cracked carbon-manganese tubes and pipes tested under pressure at 360°C, using the fracture mechanics parameters reference stress,  $\sigma_{ref}$ , stress concentration factor,  $K$ , and creep energy release rate,  $C^*$ . Residual stress measurements using the X-Ray diffraction technique and a successive layer removal method have been performed through the thickness of the pipe extrados. These data have been used in finite element analysis to model effects of the secondary stresses acting on the crack tip. Creep crack growth rates versus  $C^*$  at 360°C, in cold bent tubes, were shown to be faster by a factor of about 50 at constant  $C^*$  compared to cracking in fracture mechanics  $CT$  test specimens.

The numerical calculations of creep damage development and life behavior of circular notched specimens have been performed with the Kachanov-Rabotnov damage Law [4]. The creep deformation will relax the elastic stress concentrations. The redistribution of the stress concentration depends on the material properties and specimen geometry.

In order to evaluate the fatigue damage of high pressure tube steel strain controlled fatigue tests using uniaxial specimens were performed by Koh [1]. The objectives of the paper were to investigate the fatigue behavior of high strength tube steel under strain-controlled conditions and evaluate its damage in the presence of mean stress by applying a cyclic strain energy density.

Studies have been carried out on carbon steel pipes to demonstrate the leak before break design criterion and validate the analytical procedures. Fatigue crack initiation, fatigue crack growth rate and fracture resistance behavior of the pipes have been experimentally and analytically evaluated [8]. A study on an axisymmetric method of creep analysis for primary and secondary creep was made by Jahed and Bidabadi [11]. Even predicting the creep life of axisymmetric problems such as gas turbine discs and pressure vessels are complex task but very important. Even the most elaborate finite element procedure provides results that are very time consuming and are not always satisfactory.

Recently, researches on creep are extended on consideration of cracked bodies. The estimations of creep fracture mechanics parameters for through-thickness cracked cylinders and finite element validation was made [44]. Wasmer et al [7] have been also studying the creep crack initiation and growth in thick section steel pipes under internal pressure. In their study they investigate the creep crack growth in pre-cracked straight and bent pipes of a 9% Cr-steel, containing multiple cracks and tested at 625° C under static and slow cyclic pressure loading.

In this thesis, an analysis and computation technique is developed for the evaluation of small axisymmetric creep deformation of boiler tubes. Three general methods are discussed, and the finite element method is proposed for best handling of calculation of creep deformations in a general complex structural components.

## **2.2 Organization of the Thesis**

In chapter one, the main causes for boiler tubes failure are shortly discussed. Then the basic assumptions employed for our creep analysis are discussed. The review of literatures is summarized on the second chapter. The mathematical modeling and basic theory of creep are discussed in the third chapter. The derivation and solution techniques are presented in chapter four. The results obtained and their discussions are included in fifth chapter. Finally the conclusion and recommendations for future research are mentioned the last chapter.

### 3. Mathematical Modeling

#### 3.1 Introduction

Many pressure vessels and other engineering structures are subjected simultaneously to the action of stress and high temperature. This is the case for vessels and piping used in nuclear power plants, boilers, and chemical processing industries. The continual increase in the temperatures of operation has placed great practical importance on the strength of materials at elevated temperatures, and the development of materials to cope with this trend.

Experiments show that the yield point and the ultimate strength of a metal in tension depend considerably on the temperature [34]. Several tensile test diagrams for medium-carbon steel at different temperature show that up to about  $250^{\circ}C$  the ultimate strength of the steel increases, but with further increase in temperature it drops off rapidly. Also the yield point becomes less pronounced as the temperature increases and at the same time there is a decrease in the slope of the straight portions of the diagrams; hence decrease in modulus of elasticity.

Experiments at high temperature show that the results of tensile tests also depend on the duration of the test. As the duration of the tensile test increases, the load necessary to produce fracture becomes smaller and smaller. Experience shows that under such conditions a continuous deformation or creep takes place, which is an important factor to be considered in design.

In most experiments pertaining to creeping, the gradual elongation of a material under prolonged tension is studied. In studying the progressive creep of tensile test specimens under constant load and high temperature, two phenomena must be kept in mind:

- i.* hardening of the material due to plastic strain, and
- ii.* removal of this hardening, or “softening” of the material, due to the prolonged action of the high temperature.

In general, the strength properties (yield point and ultimate strength) decrease with high temperature while the ductile properties (elongation and reduction in area) increase. At these elevated temperatures the ultimate elongation does not always continue to increase with a rise in temperature, but reaches a peak and falls rapidly thereafter to final rupture.

We can model a boiler tube as a thick wall cylinder subjected to internal and/or external pressure at a temperature in the creep range. Thus the problem may be simplified to determine the stresses in the tube wall and analyze the failure with regard to creep deformation.

For our analysis, we will start by considering a normal boiler tube surface, i.e. surface with no soot or scale deposit and no crack and scar existing. Based on the developed model constitutive governing equation will be derived. Then the stresses and strains due to thermal loading, external load and elastic creep phenomenon will be determined by three distinct methods. These methods will be discussed in the next chapter. Further we may extend our analysis to tubes with circumferential and longitudinal through-crack on the

surface and will see some proposed relations. First let us identify the different stress categories to clarify our modeling and analysis.

## **3.2 Stress Categories**

According to the ASME stress categories, the total elastic stress which occurs in the vessel and tube shells are considered to be composed of three different types of stresses, primary, secondary, and peak [32].

### **i. Primary Stresses**

A primary stress is a stress produced by mechanical loading only and is so distributed in the structure. It is a normal stress or a shear stress developed by the imposed loading that is necessary to satisfy the simple laws of equilibrium of external and internal forces and moments. Primary stresses that considerably exceed the yield strength will result in failure, or at least in gross distortion. Typical examples of general primary stress are the average stress in a cylindrical or spherical shell due to internal pressure or due to distributed live loads, the bending stress of a flat cover without supporting moment at the periphery due to internal pressure.

### **ii. Secondary Stresses**

Secondary stresses are stresses developed by constraints due to geometric discontinuities, by the use of materials of different elastic moduli under external loads, or by constraints due to differential thermal expansion. Examples of secondary stresses are the bending stresses at dished end to shell junctions, general thermal stresses, etc.

### **iii. Peak stresses**

Peak stress is that increment of stress which is additive to the primary-plus-secondary stresses by reason of local discontinuities or local thermal stress including the effects (if any) of stress concentration. A typical example is the stress at the weld toe, crack, scar, etc.

Failure of pressure vessel and piping system that operate at high temperature can occur by *net section rupture*, *creep crack growth* or a combination of both processes. In the case of boiler tubes, overheating and overloading of the tube will cause net section rupture. Scale formation on the tube wall or shortage of feed waters will affect the heat transfer processes, so that net section rupture may happen due to overheating. Improperly working safety and drainage valves will cause pressure build-up inside the tube and thus lead to probable net section rupture due to high pressure.

On the other hand boiler tubes are subjected to erosion and corrosion that cause tubes to become locally thinned or scarred and cracked. Scars and cracks are known to facilitate the creep failure. Operational boiler tubes may experience cyclic thermal, pressure and system loadings between long periods of normal and steady-state operation. During so-called steady-state operation, the tube may also be subjected to high-cycle fatigue owing to fluctuating temperature and pressure. For a boiler tube in steady state operation temperature, we may neglect the damage due to temperature fatigue.

For components operating at temperatures below creep range, the design stress is based on the conventional stress analysis (yield and/ or ultimate tensile strength) of materials. But for components operating within the creep range of temperatures, the design stress is also

required to be less than or equal to the creep rupture stress for a specified life. It is normally assumed that the material damage due to *fatigue*, *plasticity* and *creep* can be estimated separately and then summed to obtain the total damage.

A structural element in creep may rupture in any of the two modes of failure, namely, *ductile* and *brittle* [21]. When a structural component is subjected to high stress levels, a failure may occur due to the geometric instability caused by necking. Such a failure would be called ductile failure. On the other hand, structures at low stresses and high temperature may exhibit brittle failure. Fissures and voids are usually found where such a failure occurs and they grow on planes which are perpendicular to the direction of the maximum principal stress.

### **3.3 Basic Theories and Assumptions**

#### **3.3.1 Theoretical background**

Modern structural elements are subjected to temperature changes which frequently result in the development of transient stresses large enough to cause plastic flow, and to elevated temperatures which often lead to creeping phenomena. In the analysis of thermal stresses in these elements the actual properties of the material cannot be described precisely without taking into consideration the following properties [34]:

- i.* temperature dependence of material properties;
- ii.* plastic deformation, considering the decrease in yield stress of the material with rising temperature; and
- iii.* time-dependent strain and stress response of materials.

At elevated temperatures the deformation of metals continues with no increase in stress. This is called *creep* and is defined as the time dependent inelastic deformation of materials [21, 22]. Creep properties are obtained by subjecting tensile specimens to a constant load at a constant temperature and observing the axial strain at selected time intervals.

### 3.3.2 Creep Curves at Constant Stress

It has been found from experiment that if a metal which creeps is subjected to a constant uniaxial stress then the accumulation of creep strains with time has the form illustrated in as shown by Fig. 3.1 [38, 41]. The variation of strain with time is described by the following stages.

**OA** is an instantaneous deformation that occurs immediately upon application of the load and may contain both elastic and plastic deformation.

**AB** is the primary stage in which creep changes at a decreasing rate as a result of strain hardening. The deformation is mainly plastic.

**BC** is the secondary steady state stage in which the deformation is plastic. In this stage the creep rate reaches a minimum and remains constant as the effect of strain-hardening is counter balanced by an annealing influence. Here the creep rate is a function of stress level and temperature.

**CD** is the tertiary stage in which the creep continues to increase and is also accompanied by a reduction in cross-sectional area and the onset of necking, hence increase in necking, thereby resulting in fracture.

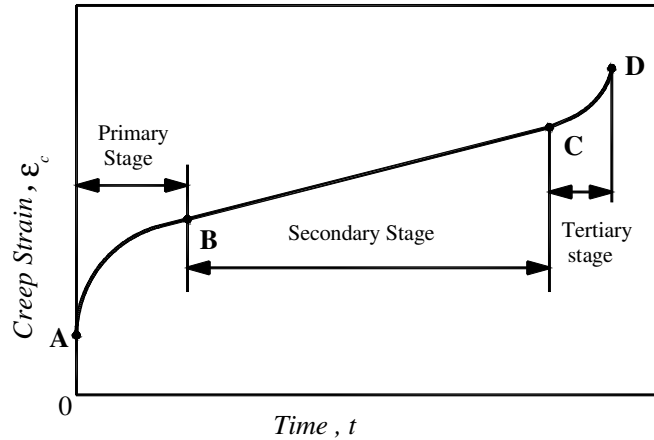


*Fig. 3.1 Creep curve obtained at constant temperature under constant load*

### 3.3.3 Basic Assumptions

Operational boiler tubes may be considered as long, thick-walled cylindrical tubes which are subjected to internal and/or external pressure and operating at elevated temperatures. Thus, a boiler tube may undergo elastic, plastic and/or creep deformations. To make analysis of these factors, we consider an axisymmetric hollow circular cylinder of inner and outer radii  $a$  and  $b$  respectively under the following assumptions [27].

- i.* The deformation is small and the radius of the deformed cylinder is nearly the same as the radius of the non deformed cylinder.
- ii.* The material is homogeneous, isotropic and compressible.
- iii.* All material properties are temperature dependnt (for creep analysis).
- iv.* Prandtl-Reuss work-hardening flow rule, Von Mises yield criterion and Ramberg-Osgood equations are applicable.
- v.* The Mises-Mises type theory of creep and Norton's Law for creep are applicable.
- vi.* Inertia forces and the coupling term in the governing equations are neglected and plane-strain condition is valid.

### 3.4 Derivation of Equilibrium Equation

We have already modeled the boiler tube as a thick-wall cylinder which is subjected to internal and/or external pressure and used at a temperature that may induce creep. Further we may consider the ends of the boiler tube to be constrained rigidly by end plates. Therefore, we may assume the longitudinal strain is negligible and hence the tube is in state of plane strain. Not only due to the end constraint but also since the length of the cylinder is large as compared to its cross sectional dimensions, the axial strain is negligible and the cylinder is then in a state of plane strain. Assuming isotropic material properties, we may start from equilibrium consideration of an infinitesimal element taken from the tube.

If a circular cylinder of constant wall thickness is subjected to the action of uniformly distributed internal and external pressure, the deformation produced is symmetrical about the axis of the cylinder and does not change along its length. Consider an element cut from the cylinder by two planes perpendicular to the axis and at a unit distance apart as shown in Fig. 3.2. From the condition of symmetry it follows that there are no shearing stresses on the sides of an element  $PQSR$  of this element.

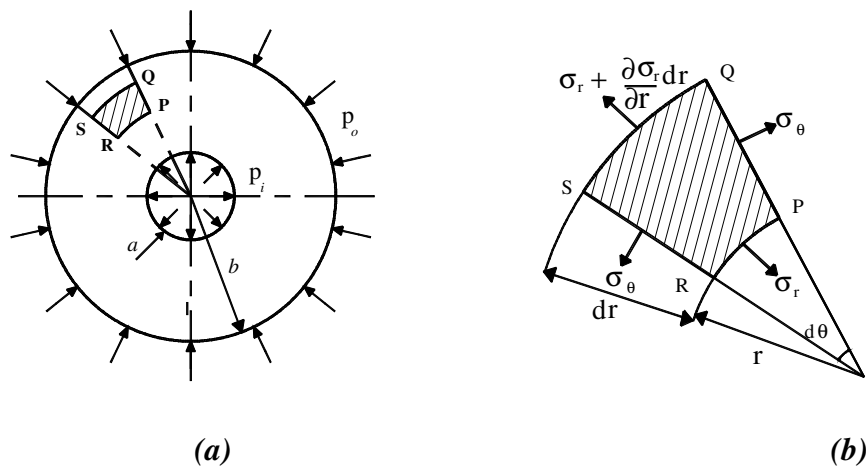


**Fig. 3.2** Pressure loading and force equilibrium diagram

Let  $\sigma_\theta$  denote the hoop-stress acting normal to the side  $PQ$  and  $RS$  of the element, and  $\sigma_r$  the radial stress normal to the side  $PR$ . The radial stress varies with the radius  $r$  and changes by an amount  $\frac{d\sigma_r}{dr}$  in the distance  $dr$ . Thus, the normal radial stress on  $QS$  is consequently:

$$\sigma_r + \frac{d\sigma_r}{dr} dr \quad (3.1)$$

Summing up the forces on the element in the direction of the bisector of the angle  $d\theta$  gives us the following equation of equilibrium

$$\sigma_r r d\theta + \sigma_\theta dr d\theta - \left( \sigma_r + \frac{d\sigma_r}{dr} dr \right) (r + dr) d\theta = 0 \quad (3.2)$$

and, neglecting higher order differentials,

$$\frac{d\sigma_r}{dr} + \frac{\sigma_r - \sigma_\theta}{r} = 0 \quad (3.3)$$

### 3.4.1 Creep Strain

Creep strain components are obtained from Norton's law [27], which assumes a power law relation to exist between the equivalent stress and equivalent strain. This is given by the equation

$$\mathcal{E}_{creep} = K \sigma_e^n t^q \quad (3.4)$$

Where  $q, n, K$ , are material constants, and  $\sigma_e$  and  $t$  are the stress and time parameter, respectively. Thus, the problem is more simplified since it is a matter of determining the stresses and the strains in the tube wall and analyzing failure with regard to plasticity and creeping. Creep problems are treated in a manner essentially similar to that for plastic-flow

problems [27, 46]. A series of computations are made, each at a progressively increasing time interval after the initiation of loading. Each computation determines the increase in creep strain during the increment in time from the previous computation. As time increases while the load is applied, two important relations must first be postulated for the computation of creep deformation.

- i.* The stress-strain-time relations as given by equation (3.4) and
- ii.* The cumulative-creep laws in cases involving variable stress history.

When the applied load is kept constant the stress-strain-time relation is assumed to have a relation given by equation (3.4), but in the case of variable load the stress-strain-time relation is determined by the cumulative creep laws. Next let us see the assumptions behind cumulative creep laws.

### **3.4.2 Cumulative Creep Laws**

Failure due to creep rupture is an important design consideration under constant stresses and temperature conditions. Expected service life can be established from standard creep rupture data. However, since most members are not subject to either constant stress or constant temperature, creep-rupture damage criteria which will predict time to rupture in such members having multi-axial states of stress using time to rupture data obtained from tension tests have evolved.

Consider first the case of uniaxial stressing in which the magnitude of the stress is varied during the test. If the stress is changed after a certain amount of creep at a given constant

stress, a question arises as to what the continuing strain-time path will be. The answer to this question has not been completely resolved, but the computation procedure can be applied to any arbitrary law. Three cumulative-creep laws that have been considered are shown next [27, 28].

**a) Time-hardening Rule**

The time-hardening rule states that the principal factor governing the creep rate is length of time at the particular temperature involved, regardless of the stress history. Let the stress be maintained at  $\sigma_5$  for the first  $t_0$  hours see Fig. 3.3, the initial creep curve being  $OA$ . If the stress is suddenly changed to  $\sigma_4$ , where  $\sigma_4 < \sigma_5$ , a new point  $A'$  is located on the  $\sigma_4$  curve vertically below  $A$  and creep proceeds along  $A'B$ . This process is repeated for  $\sigma_3$ ,  $\sigma_2$  and  $\sigma_1$ .

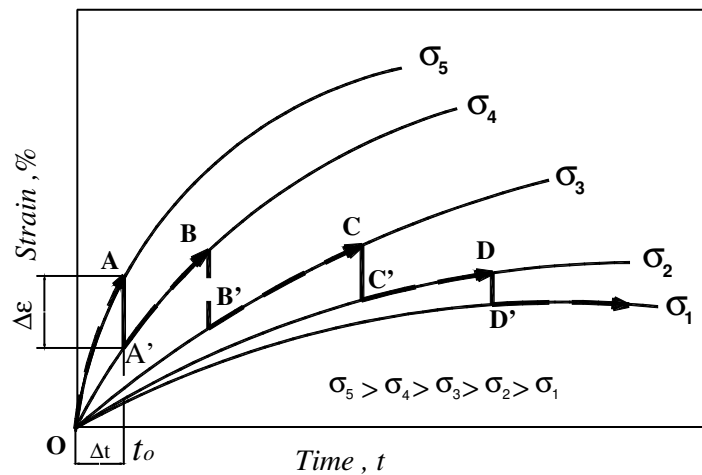


**Fig. 3.3** Time-hardening principle

If  $t_o$  represents the time at the beginning of a creep interval, equation (3.4) can now be solved for  $\sigma_e$  by replacing the time  $t$  by the average time  $t + \frac{\Delta t}{2}$  during the interval  $\Delta t$ .

Thus,

$$\sigma_e = \left( \frac{\Delta \mathcal{E}_e^c}{qK\Delta t} \right)^{\frac{1}{n}} \left( t + \frac{\Delta t}{2} \right)^{\frac{1-q}{n}} \quad (3.5)$$

### b) Strain-hardening Rule

An alternative hypothesis is the strain-hardening rule. Here the assumption is that the principal factor governing the creep rate is the strain, regardless of the stress history required to produce the strain. Thus, under variable-stress history corresponding points on new stress curve are obtained by proceeding along horizontal lines (constant strain), as indicated on Fig. 3.4. To obtain the relation between the stress, strain, and strain increment, time is eliminated between equation (3.4) and (3.5). Thus if  $\mathcal{E}_{e,o}^c$  is the equivalent creep strain at the beginning of the interval  $\Delta t$  in which the stress is changed to  $\sigma_e$  and  $\Delta \mathcal{E}_e^c$  is the increment in equivalent creep strain during the interval, the resulting relation becomes

$$\sigma_e = K^{-\frac{1}{m}} \left( \frac{\Delta \mathcal{E}_e^c}{q\Delta t} \right)^{\frac{q}{n}} \left( \mathcal{E}_{e,o}^c + \frac{\Delta \mathcal{E}_e^c}{2} \right)^{\frac{1-q}{n}} \quad (3.6)$$

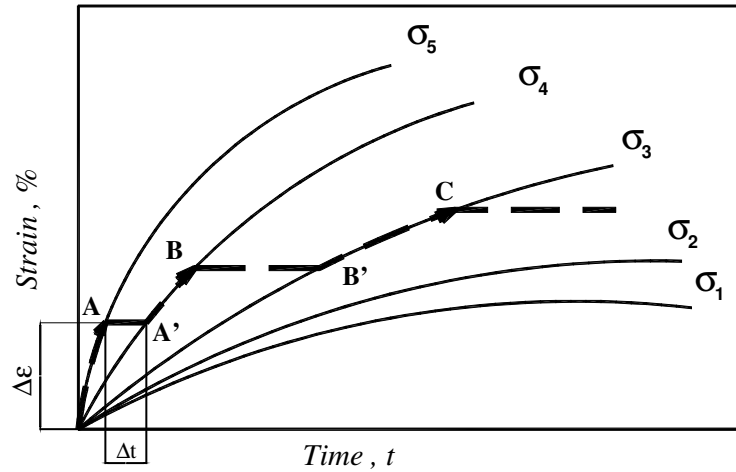


**Fig. 3.4** Strain-hardening principle

The “strain-fraction” (strain-hardening) rule is expressed by the relation

$$\sum \frac{\varepsilon_i}{\varepsilon_{li}} = 1 \quad (3.7)$$

Where  $\varepsilon_i$  is the strain for a given stress and temperature, and  $\varepsilon_{li}$  is the strain at rupture under the same stress and temperature.

### c) Life-hardening Rule

The life-fraction rule is a compromise between the time-hardening rule and the strain-hardening rule. If, for example in Fig. 3.5 creep occurs up to point  $B$  at  $\sigma_4$  and the stress is then changed to  $\sigma_3$ , the point  $B'$  is located such that the time at  $B'$  is the same function of the total life at a steady stress  $\sigma_3$  as the time at  $B$  for a steady stress  $\sigma_4$ . Thus, if the time at  $B$  is  $\frac{1}{4}$  the total life of a steady-stress at  $\sigma_4$ ,  $B'$  is chosen at  $\frac{1}{4}$  the life along the  $\sigma_3$  curve.

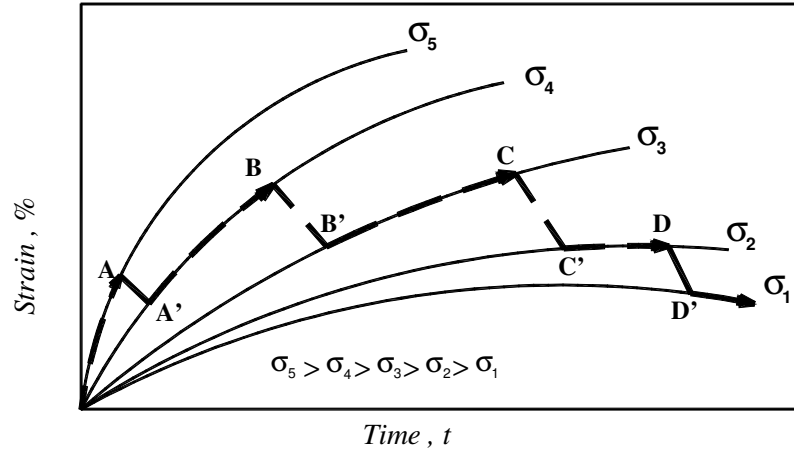


**Fig. 3.5** Time-fraction principle

The “life-fraction” rule is based on the premise that the expenditure of each individual rupture life-fraction of the total life at elevated temperature is independent of all other fractions of the life to rupture, and that when the fractional life used up at different stress levels and temperatures is added up, it will equal unity; i.e.,

$$\sum \frac{t_i}{t_{ii}} = 1 \tag{3.8}$$

Where  $t_i$  is the time at stress or temperature  $i$  and  $t_{ii}$  is the creep rupture time at temperate  $i$ .

### 3.4.3 Elastic strain

Fig. 3.6a shows an axisymmetric ring element and its cross-section to represent the general state of strain for an axisymmetric problem. It is most convenient to express the displacements of an element  $PQSR$  in the plane of cross-section in polar coordinates. We then let  $u$  and  $w$  denote the displacements in the radial and longitudinal directions, respectively. The side  $PR$  of the element is displaced an amount  $u$  and side  $QS$  is then

displaced an amount  $u + \frac{\partial u}{\partial r} dr$  in the radial direction. The normal strain in the radial direction is then given by

$$\varepsilon_r = \frac{\partial u}{\partial r} \quad (3.9a)$$

In general, the strain in the tangential direction depends on the tangential displacement  $v$  and on the radial displacement  $u$ . However, for axisymmetric deformation behavior, recall that the tangential displacement  $v$  is equal to zero. Hence, the tangential strain is due to only to the radial displacement. Having only radial displacement  $u$ , the new length of the arc  $PR$  is  $(r + u) d\theta$ , and the tangential strain is then given by

$$\varepsilon_\theta = \frac{(r + u) d\theta - r d\theta}{r d\theta} = \frac{u}{r} \quad (3.9b)$$

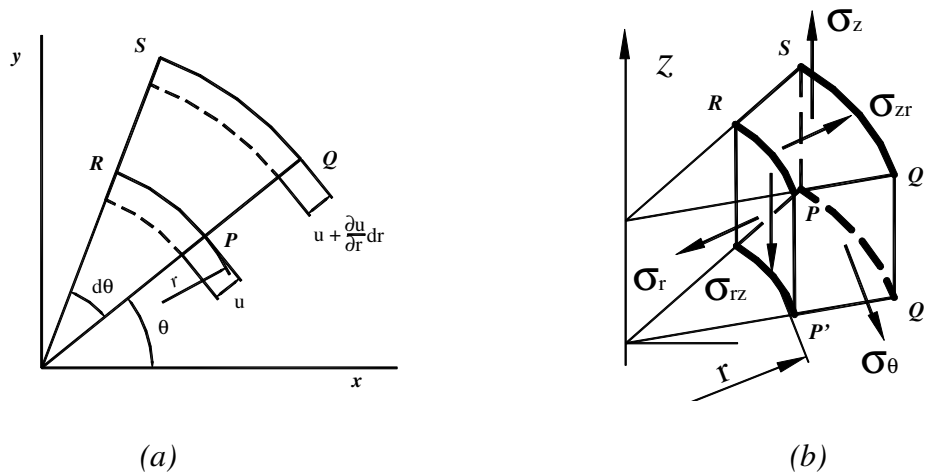


**Fig. 3.6** Cross-section of axisymmetric element

Next, we consider the longitudinal element  $PQQ'P'$  to obtain the longitudinal strain and the shear strain. In Fig. 3.6b, the element is shown to be displaced by amounts  $u$  and  $w$  in the radial and longitudinal directions at point  $P'$ , and to displace additional amounts  $\frac{\partial w}{\partial z} dz$ .

along line  $PP'$  and  $\frac{\partial u}{\partial r} dr$  along lines  $P'Q'$ . Furthermore, observing line  $P'Q'$  and  $PP'$ , we

see that the point  $Q'$  moves upward an amount  $\frac{\partial w}{\partial r} dr$  with respect to point  $P'$  and point  $P$

moves to the right an amount  $\frac{\partial u}{\partial z} dz$  with respect to point  $P'$ . Again, from the basic

definitions of normal and shear strain, we have the longitudinal normal strain given by

$$\epsilon_z = \frac{\partial w}{\partial z} \quad (3.9c)$$

and the shear strain in the  $r - z$  plane given by

$$\epsilon_{rz} = \frac{\partial u}{\partial z} + \frac{\partial w}{\partial r} \quad (3.9d)$$

From Hooke's law the expressions for the stresses in terms of the strains are

$$\sigma_r = \frac{E}{1-\nu^2} \left( \frac{du}{dr} + \nu \frac{u}{r} \right) \quad (3.10a)$$

$$\sigma_\theta = \frac{E}{1-\nu^2} \left( \frac{u}{r} + \nu \frac{du}{dr} \right) \quad (3.10b)$$

Substituting equations (3.10a and 3.10b) into the equation for equilibrium, equation (3.2)

we obtain the following equation for determining  $u$

$$\frac{d^2 u}{dr^2} + \frac{1}{r} \frac{du}{dr} - \frac{u}{r^2} = 0 \quad (3.11)$$

The general solution for this equation is

$$u = C_1 r + \frac{C_2}{r} \quad (3.12)$$

Where  $C_1$  and  $C_2$  are integration constants to be determined from boundary conditions.

Substituting equation (3.14) into equation (3.12a and 3.12b)

$$\sigma_r = \frac{E}{1-\nu^2} \left[ C_1(1+\nu) - C_2 \frac{(1-\nu)}{r^2} \right] \quad (3.13a)$$

$$\sigma_\theta = \frac{E}{1-\nu^2} \left[ C_1(1+\nu) + C_2 \frac{(1-\nu)}{r^2} \right] \quad (3.13b)$$

If  $p_i$  and  $p_o$  denote the internal and external pressures respectively, the conditions at the outer and inner surfaces of the cylinder are

$$(\sigma_r)_{r=b} = -p_o \quad \text{and} \quad (\sigma_r)_{r=a} = -p_i$$

Therefore,

$$C_1 = \frac{1-\nu}{E} \frac{a^2 p_i - b^2 p_o}{b^2 - a^2} \quad \text{and} \quad C_2 = \frac{1+\nu}{E} \frac{a^2 b^2 (p_i - p_o)}{b^2 - a^2}$$

With these values for the integration constants, the general expression for the normal stresses  $\sigma_r$ ,  $\sigma_\theta$  and radial deformation  $u$  become

$$\sigma_r = \frac{a^2 p_i - b^2 p_o}{b^2 - a^2} - \frac{(p_i - p_o) a^2 b^2}{r^2 (b^2 - a^2)} \quad (3.14a)$$

$$\sigma_\theta = \frac{a^2 p_i - b^2 p_o}{b^2 - a^2} + \frac{(p_i - p_o) a^2 b^2}{r^2 (b^2 - a^2)} \quad (3.14b)$$

$$u = C_1 r + \frac{C_2}{r} = \frac{1-\nu}{E} \frac{a^2 p_i - b^2 p_o}{b^2 - a^2} r + \frac{1+\nu}{E} \frac{a^2 b^2 (p_i - p_o)}{b^2 - a^2} \frac{1}{r} \quad (3.15)$$

Therefore, the elastic strains are

$$\epsilon_r = \frac{du}{dr} = \frac{1-\nu}{E} \frac{a^2 p_i - b^2 p_o}{b^2 - a^2} - \frac{1+\nu}{E} \frac{a^2 b^2 (p_i - p_o)}{b^2 - a^2} \frac{1}{r^2} \quad (3.16a)$$

$$\epsilon_\theta = \frac{u}{r} = \frac{1-\nu}{E} \frac{a^2 p_i - b^2 p_o}{b^2 - a^2} + \frac{1+\nu}{E} \frac{a^2 b^2 (p_i - p_o)}{b^2 - a^2} \frac{1}{r^2} \quad (3.16b)$$

### 3.4.4 Thermal Strains

When the wall of a cylinder is heated non-uniformly, its elements do not expand uniformly and mutual interference sets up thermal stresses. In the following discussion the distribution of the temperature is taken to be symmetrical with respect to the axis of the cylinder.

During thermal deformation such cross sections can be assumed to remain plane if taken sufficiently distant from the ends of the cylinder, hence the unit elongations in the direction of the axis are constant as expressed by equation (3.9a-3.9d). These elongations can be represented as functions of the stresses  $\sigma_z, \sigma_r, \sigma_\theta$  and the thermal expansion,  $\alpha$ . Let the temperature difference above the minimum temperature on the tube at each radial point is given by  $T$  and assume varies with the radial distance  $r$ , only,

$$\varepsilon_z = \frac{\sigma_z}{E} - \frac{\nu}{E}(\sigma_r + \sigma_\theta) + \alpha T \quad (3.17a)$$

$$\varepsilon_r = \frac{\sigma_r}{E} - \frac{\nu}{E}(\sigma_z + \sigma_\theta) + \alpha T \quad (3.17b)$$

$$\varepsilon_\theta = \frac{\sigma_\theta}{E} - \frac{\nu}{E}(\sigma_z + \sigma_r) + \alpha T \quad (3.17c)$$

Using the symbol  $\Lambda$  for the unit increase in volume, we obtain

$$\Lambda = \varepsilon_z + \varepsilon_r + \varepsilon_\theta = \frac{1 - 2\nu}{E}(\sigma_z + \sigma_r + \sigma_\theta) + 3\alpha T \quad (3.18)$$

By substituting equations (3.17) into equations (3.10) and use equation (3.18) for further simplification we obtain

$$\sigma_z = \frac{E}{1 + \nu} \left[ \varepsilon_z + \frac{\nu}{1 - 2\nu} \Lambda \right] - \frac{E}{1 - 2\nu} \alpha T \quad (3.19a)$$

$$\sigma_r = \frac{E}{1+\nu} \left[ \epsilon_r + \frac{\nu}{1-2\nu} \Lambda \right] - \frac{E}{1-2\nu} \alpha T \quad (3.19b)$$

$$\sigma_\theta = \frac{E}{1+\nu} \left[ \epsilon_\theta + \frac{\nu}{1-2\nu} \Lambda \right] - \frac{E}{1-2\nu} \alpha T \quad (3.19c)$$

Substituting equation (3.18) and equations (3.19) into equations of equilibrium, equation (3.2), we get

$$\frac{d^2u}{dr^2} + \frac{1}{r} \frac{du}{dr} - \frac{u}{r^2} = \frac{d}{dr} \left[ \frac{1}{r} \frac{d}{dr} (ru) \right] = \frac{1+\nu}{1-\nu} \alpha \frac{dT}{dr} \quad (3.20)$$

Thus,

$$u = \frac{1}{r} \left( \frac{1+\nu}{1-\nu} \right) \int_a^r \alpha T r dr + C_1^* r + \frac{C_2^*}{r} \quad (3.21)$$

Where  $C_1^*$  and  $C_2^*$  are integration constants. If the inner and exterior surfaces are free from external forces, we can apply the following boundary conditions

B.C  $(\sigma_r)_{r=a} = 0$  and  $(\sigma_r)_{r=b} = 0$ , Thus

$$\sigma_r = \frac{\alpha E}{1-\nu} \frac{1}{r^2} \left( \frac{r^2 - a^2}{b^2 - a^2} \int_a^b T r dr - \int_a^r T r dr \right) \quad (3.22a)$$

$$\sigma_\theta = \frac{\alpha E}{1-\nu} \frac{1}{r^2} \left( \frac{r^2 + a^2}{b^2 - a^2} \int_a^b T r dr + \int_a^r T r dr - T r^2 \right) \quad (3.22b)$$

$$\sigma_z = \frac{\alpha E}{1-\nu} \left( \frac{2}{b^2 - a^2} \int_a^b T r dr - T \right) \quad (3.22c)$$

Usually for thick wall tubes logarithmic temperature distribution is assumed. Let the temperature at the inner surface and outer surface are given as  $T_i$  and  $T_o$  respectively. If we assume  $T_i > T_o$  and the temperature difference between the inner and external surface  $\Delta T = T_i - T_o$ , the distribution of temperature through the wall is given by

$$T(r) = T_i + \Delta T \frac{\ln\left(\frac{a}{r}\right)}{\ln\left(\frac{b}{a}\right)} \quad (3.23)$$

Therefore,

$$\sigma_r = \frac{\alpha E \Delta T}{2(1-\nu) \ln\left(\frac{b}{a}\right)} \left[ -\ln\left(\frac{b}{r}\right) - \frac{a^2}{b^2 - a^2} \left(1 - \frac{b^2}{r^2}\right) \ln\left(\frac{b}{a}\right) \right] \quad (3.24a)$$

$$\sigma_\theta = \frac{\alpha E \Delta T}{2(1-\nu) \ln\left(\frac{b}{a}\right)} \left[ 1 - \ln\left(\frac{b}{r}\right) - \frac{a^2}{b^2 - a^2} \left(1 + \frac{b^2}{r^2}\right) \ln\left(\frac{b}{a}\right) \right] \quad (3.24b)$$

$$\sigma_z = \frac{\alpha E \Delta T}{2(1-\nu) \ln\left(\frac{b}{a}\right)} \left[ 1 - 2 \ln\left(\frac{b}{r}\right) - \frac{2a^2}{b^2 - a^2} \ln\left(\frac{b}{a}\right) \right] \quad (3.25c)$$

Note if there is no temperature gradient through the tube or  $\Delta T = 0$ ;  $\sigma_r = \sigma_\theta = \sigma_z = 0$

### 3.4.5 Total strain

Total strains are assumed to be composed of three parts: elastic, thermal and creep strain

Hamid J. et al [11]. Mathematically the total strain can be written as

$$\varepsilon_{total} = \varepsilon_{elastic} + \varepsilon_{thermal} + \varepsilon_{creep} \quad (3.26)$$

## 4 Solution Technique

### 4.1 Analytical Approach

In the absence of additional experimental information regarding creep under combined stress, it is necessary to adapt the result of a simple-tension creep tests to the solution of more complicated problems [27, 34]. This is usually accomplished by assuming that:

- i.* during creep and plastic deformation, the direction of the principal stresses,  $\sigma_1$ ,  $\sigma_2$  and  $\sigma_3$ , coincide with the direction of the principal strains  $\epsilon_1$ ,  $\epsilon_2$  and  $\epsilon_3$ ;
- ii.* the volume of the material remains constant, so that for small deformations  $\epsilon_1 + \epsilon_2 + \epsilon_3 = 0$ ; and (4.1)
- iii.* the maximum shearing stresses are proportional to the corresponding shearing strains.

It can be shown that the values of shearing strain on the planes bisecting the angles between the principal planes are  $\epsilon_1 - \epsilon_2$ ,  $\epsilon_2 - \epsilon_3$  and  $\epsilon_3 - \epsilon_1$ . In order to obtain this result let us consider a cubic element shown in Fig. 4.1 having unit elongations  $\epsilon_1$  and  $\epsilon_2$  in the directions 1 and 2.

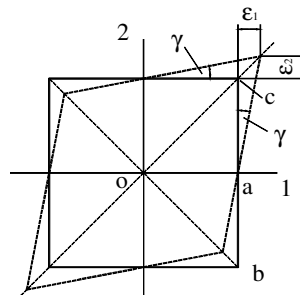


**Fig. 4.1** Simple cubic element

The shearing strain  $\varepsilon_{12} = 2\gamma$  corresponding to the planes  $ob$  and  $oc$  are found from the triangle  $oab$ . Assuming that  $\varepsilon_1 > \varepsilon_2$ , we obtain

$$\tan\left(\frac{\pi}{4} - \frac{\varepsilon_{12}}{2}\right) \approx \frac{1-\gamma}{1+\gamma} = \frac{1+\varepsilon_2}{1+\varepsilon_1} \quad (4.2)$$

From which

$$\varepsilon_{12} = \varepsilon_1 - \varepsilon_2 \quad (4.3)$$

Similarly, we can find the shearing strains for the other two bisection planes, and assumption (3) then takes the following form

$$\frac{\varepsilon_1 - \varepsilon_2}{\sigma_1 - \sigma_2} = \frac{\varepsilon_2 - \varepsilon_3}{\sigma_2 - \sigma_3} = \frac{\varepsilon_3 - \varepsilon_1}{\sigma_3 - \sigma_1} = \xi \quad (4.4)$$

Where  $\xi$  is a function of  $\sigma_1, \sigma_2$  and  $\sigma_3$  which must be determined from experiments.

From equation (4.1) and equation (4.4) it follows that [41]

$$\varepsilon_1 = \frac{2\xi}{3} \left[ \sigma_1 - \frac{1}{2}(\sigma_2 + \sigma_3) \right] \quad (4.5a)$$

$$\varepsilon_2 = \frac{2\xi}{3} \left[ \sigma_2 - \frac{1}{2}(\sigma_1 + \sigma_3) \right] \quad (4.5b)$$

$$\varepsilon_3 = \frac{2\xi}{3} \left[ \sigma_3 - \frac{1}{2}(\sigma_2 + \sigma_1) \right] \quad (4.5c)$$

To adapt equations (4.5) to creep at a constant rate, we can divide these equations by the time  $t$ . Using the notations  $\dot{\varepsilon}_1, \dot{\varepsilon}_2$  and  $\dot{\varepsilon}_3$  for the principal creep rates and denoting the factors before the brackets by  $\Psi$ , we arrive at the following equations

$$\dot{\varepsilon}_1 = \Psi \left[ \sigma_1 - \frac{1}{2}(\sigma_2 + \sigma_3) \right] \quad (4.6a)$$

$$\dot{\varepsilon}_2 = \Psi \left[ \sigma_2 - \frac{1}{2}(\sigma_1 + \sigma_3) \right] \quad (4.6b)$$

$$\dot{\epsilon}_3 = \Psi \left[ \sigma_3 - \frac{1}{2}(\sigma_1 + \sigma_2) \right] \quad (4.6c)$$

Applying these equations to simple tension model, where  $\sigma_1 = \sigma$  and  $\sigma_2 = \sigma_3 = 0$ , we obtain

$$\dot{\epsilon} = \Psi \sigma \quad (4.7)$$

The primary region is of greater interest for structures subjected to cyclic loading [38], the period of loading being of the same order as the time during which primary creep takes place. It is found that the primary portion of the creep curve is adequately described by an equation of the following type [41]

$$\epsilon = K \sigma^n t^q \quad (4.8)$$

where  $K$  and  $n$  are constants depend on the metal,  $n$  is normally being between 2 and 9 and  $q$  is normally about 0.33.

The portion of interest of the creep curve Fig. 3.1 depends upon the problem under consideration. For example in the traditional situation of steady loads sustained for long periods, the problem has been the determination of long-term deformations [38, 40]. In this situation the elastic and primary portions of the curves are usually neglected as being small with respect to the steady-state creep and the simplified creep curves and the simplified creep curves take the form shown by Fig. 4.2. It is found that the steady-state creep rate ( $q = 1$ ) is governed by a formula of the type

$$\frac{d\epsilon}{dt} = K \sigma^n \quad (4.9)$$

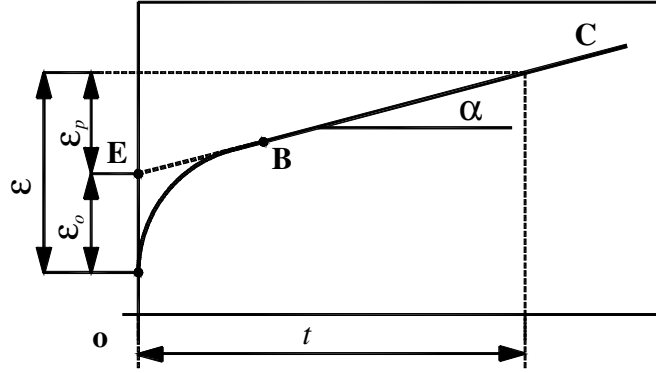


**Fig. 4.2** Simplified creep curve at constant temperature under constant load

To bring equation (4.7) and equation (4.9) into agreement, we must take

$$\Psi = K\sigma^{n-1} \quad (4.10)$$

To establish the form of the function  $\Psi$  for the general case of creep, represented by equation (4.6), we use the Von Misses yielding condition for a three-dimensional stress system and for simple tension [31, 34]. Introducing the value of equivalent stress

$$\sigma_e = \frac{1}{\sqrt{2}} \sqrt{(\sigma_1 - \sigma_2)^2 + (\sigma_2 - \sigma_3)^2 + (\sigma_3 - \sigma_1)^2} \quad (4.11)$$

Equations (4.6) then become

$$\dot{\epsilon}_1 = K\sigma_e^{n-1} \left[ \sigma_1 - \frac{1}{2}(\sigma_2 + \sigma_3) \right] \quad (4.12a)$$

$$\dot{\epsilon}_2 = K\sigma_e^{n-1} \left[ \sigma_2 - \frac{1}{2}(\sigma_1 + \sigma_3) \right] \quad (4.12b)$$

$$\dot{\epsilon}_3 = K\sigma_e^{n-1} \left[ \sigma_3 - \frac{1}{2}(\sigma_1 + \sigma_2) \right] \quad (4.12c)$$

We may make simple analogy of the above synthesis for cases of creeping boiler tubes. Let us consider thick boiler tube under internal pressure  $p$  and operating temperature  $T$ .

Assuming that the pipe is in a condition of plane strain, the axial strain  $\varepsilon_z$  vanishes and thus,

$$\dot{\varepsilon}_\theta = K\sigma_e^{n-1} \left[ \sigma_\theta - \frac{1}{2}(\sigma_r + \sigma_z) \right] \quad (4.13a)$$

$$\dot{\varepsilon}_r = K\sigma_e^{n-1} \left[ \sigma_r - \frac{1}{2}(\sigma_\theta + \sigma_z) \right] \quad (4.13b)$$

$$\dot{\varepsilon}_z = K\sigma_e^{n-1} \left[ \sigma_z - \frac{1}{2}(\sigma_r + \sigma_\theta) \right] = 0 \quad (4.13c)$$

From the last equation we conclude that

$$\sigma_z = \frac{1}{2}(\sigma_\theta + \sigma_r) \quad (4.14)$$

From the condition of equilibrium of the element shown in previous discussions equation (3.2), to determine  $\sigma_\theta$  and  $\sigma_r$  we have considered the deformation of the tube, equation (3.10) and equation (3.11). Now if we differentiate equation (3.11) with respect to  $r$ , we obtain

$$\frac{d\varepsilon_\theta}{dr} = \frac{1}{r} \frac{du}{dr} - \frac{u}{r^2} = \frac{1}{r}(\varepsilon_r - \varepsilon_\theta) \quad (4.15)$$

Assuming a steady state of creep and if we divide equation (4.15) by time  $t$ , we have

$$\frac{d\dot{\varepsilon}_\theta}{dr} = \frac{1}{r}(\dot{\varepsilon}_r - \dot{\varepsilon}_\theta) \quad (4.16)$$

Substituting for  $\dot{\varepsilon}_\theta$  and  $\dot{\varepsilon}_r$  from equations (4.13) an additional equation for determining the principal stresses is obtained. This equation can be greatly simplified by using equation (4.14). The equivalent tension then becomes

$$\sigma_e = \frac{\sqrt{3}}{2}(\sigma_\theta - \sigma_r) \quad (4.17)$$

and we obtain, from equation (4.13a) and equation (4.13b)

$$\dot{\epsilon}_{\theta} = -\dot{\epsilon}_r = K \left( \frac{\sqrt{3}}{2} \right)^{n+1} (\sigma_{\theta} - \sigma_r)^n \quad (4.18)$$

Equilibrium equation, equation (3.3) then becomes

$$\frac{d}{dr} (\sigma_{\theta} - \sigma_r)^n = -\frac{2}{r} (\sigma_{\theta} - \sigma_r)^n \quad (4.19)$$

and we conclude that

$$(\sigma_{\theta} - \sigma_r)^n = \frac{C}{r^2} \quad (4.20)$$

where C is constant of integration, and therefore

$$\frac{d\sigma_r}{dr} = \frac{1}{r} \left( \frac{C}{r^2} \right)^{\frac{1}{n}} \quad (4.21)$$

and after integration we obtain

$$\sigma_r = -\frac{n}{2} C_1 r^{-\frac{2}{n}} + C_2 \quad (4.22)$$

where  $C_1 = C^{\frac{1}{n}}$

The integration constants  $C_1$  and  $C_2$  will now be determined from the conditions at the inner and outer surface of the pipe. If we assume the tube is loaded by internal pressure only

$$(\sigma_r)_{r=a} = -p = -\frac{n}{2} C_1 a^{-\frac{2}{n}} + C_2 \quad \text{and} \quad (\sigma_r)_{r=b} = 0 = -\frac{n}{2} C_1 b^{-\frac{2}{n}} + C_2 \quad (4.23)$$

From these equations we obtain

$$C_1 = -\frac{2p}{n(b^{-\frac{2}{n}} - a^{-\frac{2}{n}})} \quad \text{and} \quad C_2 = -\frac{pb^{-\frac{2}{n}}}{b^{-\frac{2}{n}} - a^{-\frac{2}{n}}} \quad (4.24)$$

Therefore, eliminating the constants in equation (4.22) by equation (4.24) we get

$$\sigma_r = -p \frac{\left(\frac{b}{r}\right)^{\frac{2}{n}} - 1}{\left(\frac{b}{a}\right)^{\frac{2}{n}} - 1} \quad (4.25)$$

From equation (4.20) and equation (4.25) we then obtain

$$\sigma_\theta = p \frac{1 + \frac{2-n}{n} \left(\frac{b}{r}\right)^{\frac{2}{n}}}{\left(\frac{b}{a}\right)^{\frac{2}{n}} - 1} \quad (4.26a)$$

$$\sigma_z = \frac{p}{\left(\frac{b}{a}\right)^2 - 1} \left[ 1 + \left(\frac{1-n}{n}\right) \left(\frac{b}{r}\right)^{\frac{2}{n}} \right] \quad (4.26b)$$

Equations (4.14), (4.25) and (4.26) give the stresses in the pipe under conditions of steady creep rates. The magnitudes of the creep rate are obtained from equation (4.18), which gives

$$\dot{\epsilon}_\theta = -\dot{\epsilon}_r = \frac{1}{2} 3^{\frac{n+1}{2}} K \left(\frac{b}{r}\right)^2 \left(\frac{1}{n}\right)^n \left[ \frac{p}{\left(\frac{b}{a}\right)^{\frac{2}{n}} - 1} \right]^n \quad (4.27)$$

Although creep deformation may appear to be within allowable limits, this is no guarantee that failure will not occur as the condition of stress rupture may be reached [48]. The maximum tensile stress occurs at the outside surface where  $r=b$ , which gives an expression for allowable pressure as a function of geometry and  $n$ .

$$P_{rupture} = \frac{n\sigma_y}{\sqrt{3}} \left( \left(\frac{b}{a}\right)^{\frac{2}{n}} - 1 \right) \quad (4.28)$$

It is assumed in the above derivation that the temperature of the pipe does not change with  $r$ . In the next chapter simple solution will be obtained by assuming a steady state of creep. It gives satisfactory results for the creep which takes place after a long period of action of the forces. If we wish to ascertain what the creep is after only a short duration of load, the formulas derived on the assumption of steady creep are not satisfactory; we must have recourse to the creep curve  $BC$  see Fig. 4.2. The problem becomes complicated, and difficult to calculate analytically.

In the cases of temperature differential through the tube wall, with the heat flowing towards the bore, the temperature distribution under steady state condition is given by the following equation [48]

$$T = T_{mean} + \frac{HK}{k} \left( \frac{\log r}{\sqrt{a+b}} \right) \quad (4.29)$$

Where:  $H$  = Heat transfer rate at outside surface

$k$  = Thermal conductivity of the tube

$T_{mean}$  = Mean temperature through the tube

Therefore, the  $n$  in all the above stress equations can be used by substituting  $n'$ , which is defined as follows

$$n' = \frac{n}{1 + \frac{Hb}{2kK}} \quad (4.30)$$

## 4.2 Incremental Approach (Analytical)

Commonly accepted basis for design of pressure vessels at elevated temperatures has been the use of tensile secondary-creep data applied to combined steady stress. Such methods were used by Bailey, Marin, and Soderberg as we can see from Coffin et. al. [38]. The creep analysis of boiler tubes by secondary-creep data has been discussed in the preceding sections. However, in short life, secondary-creep conditions are rarely attained and primary creep must be the basis for any analysis.

Coffin et. al. [38] attempt to show how the tensile primary-creep characteristics may be utilized in the design of thick-walled pressure vessels. In other words, they attempt to trace the stress-deformation history of the tube from the time when the pressure is applied initially until its life expectancy, or to the time which the steady-state conditions corresponding to secondary creep are reached. Here we will derive a rate type governing equation to estimate the residual stress field developed in the boiler tubes. Once we have estimated the residual stress fields by simple stress-strain superposition, we can trace the instantaneous stress-strain history. Gill [36] made such analysis to predict the creep history on circular hole in a sheet subjected to uniform sheet at creeping temperature range. References are also made to Jahed and Bidabadi [11], who have used a similar approach for creep analysis in inhomogeneous rotating disc. In this thesis, an approach similar to that of Gill and Jahed will be used for boiler tube creep analysis.

### 4.2.1 Governing Equations

Our analysis has been made for a thick-walled boiler tube under constant temperature throughout the wall and isotropic material properties. Consider a differential element of an axisymmetric member which is in equilibrium. We will start from the equilibrium consideration of this element as derived in the previous chapter and given by equation (3.3), and the total strains as assumed in equation (3.29). In the case of plane strain, the compatibility equations take the following form.

$$\varepsilon_r = \frac{du}{dr} = \frac{1-\nu^2}{E}\sigma_r - \frac{\nu(1+\nu)}{E}\sigma_\theta + \alpha T + \varepsilon_r^c \quad (4.28a)$$

$$\varepsilon_\theta = \frac{u}{r} = \frac{1-\nu^2}{E}\sigma_\theta - \frac{\nu(1-\nu)}{E}\sigma_r + \alpha T + \varepsilon_\theta^c \quad (4.28b)$$

Thus, the radial and tangential stresses  $\sigma_r$  and  $\sigma_\theta$  can be determined by Hooke's law, and for plane strain state they are given by

$$\sigma_r = \frac{E}{(1-2\nu)(1+\nu)} \left[ (1-\nu) \frac{du}{dr} + \nu \frac{u}{r} - ((1-\nu)\varepsilon_r^c + \nu\varepsilon_\theta^c) - \alpha T \right] \quad (4.29a)$$

$$\sigma_\theta = \frac{E}{(1-2\nu)(1+\nu)} \left[ \nu \frac{du}{dr} + (1-\nu) \frac{u}{r} - (\nu\varepsilon_r^c + (1-\nu)\varepsilon_\theta^c) - \alpha T \right] \quad (4.29b)$$

Substituting equation (4.29) into the equilibrium equation (3.3) yields the governing equation of the form

$$\frac{d^2u}{dr^2} + \frac{1}{r} \frac{du}{dr} - \frac{1}{r^2}u = \frac{g_1}{r} + \frac{dg_2}{dr} \quad \text{where} \quad (4.30)$$

$$g_1 = \frac{1-2\nu}{1-\nu} (\varepsilon_r^c - \varepsilon_\theta^c) \quad \text{and} \quad g_2 = \varepsilon_r^c + \frac{\nu}{1-\nu} \varepsilon_\theta^c \quad (4.31)$$

If the tube is free from initial creep strain, the thermo-elastic behavior is governed by the equation

$$\frac{d^2u}{dr^2} + \frac{1}{r} \frac{du}{dr} - \frac{1}{r^2}u = 0 \quad (4.32)$$

Equation (4.32) is similar to Lamé's equation which is used to determine the strain and deformation at time  $t = 0$ . Since creep is a time dependent problem, we need to derive rate type governing equation helpful to estimate the residual stress field. Once the residual stress field is estimated the instantaneous quantities are determined by the principles of superposition. The rate type governing equation may be derived by differentiating equation (4.30) with respect to time. Hence, for time  $t > 0$ , the governing rate equation becomes

$$\frac{d^2\dot{u}}{dr^2} + \frac{1}{r} \frac{d\dot{u}}{dr} - \frac{1}{r^2}\dot{u} = \frac{\dot{g}_1}{r} + \frac{\dot{g}_2}{dr} \quad \text{where} \quad (4.33)$$

$$\dot{g}_1 = \frac{1-2\nu}{1-\nu}(\dot{\epsilon}_r^c - \dot{\epsilon}_\theta^c) \quad \text{and} \quad \dot{g}_2 = \dot{\epsilon}_r^c + \frac{\nu}{1-\nu}\dot{\epsilon}_\theta^c \quad (4.34)$$

In general, there are no exact solutions to these equations. However, there have been numerous numerical methods for the treatment of such problems. Jahed and Bidabadi [11] used axisymmetric method of creep analysis for primary and secondary creep in the time domain for creep analysis of inhomogeneous body. The method is based on estimating the residual stress field which was proposed by Jahed and Dubay earlier. Prediction of residual stress in axisymmetric homogeneous materials is relatively simple. Greenbaum and Rubinstein [37] employed the finite element analysis. For our analysis of creep in boiler tubes, next we use see the residual stress field prediction method (stepwise integration) first, and then we will make use of FEA and compare the results obtained.

Radial and tangential strain rates can be obtained from the Prantel Reuss flow rule [11]. For plain strain case. These are given by

$$\dot{\epsilon}_r^c = \frac{3}{4} \frac{\dot{\epsilon}_e}{\sigma_e} (\sigma_r - \sigma_\theta) \quad (4.35a)$$

$$\dot{\epsilon}_\theta^c = \frac{3}{4} \frac{\dot{\epsilon}_e}{\sigma_e} (\sigma_\theta - \sigma_r) = -\dot{\epsilon}_r^c \quad (4.35b)$$

where  $\sigma_e$  and  $\dot{\epsilon}_e$  are the Von Mises effective stress and the strain rate, respectively. The general solution of equation (4.33) is

$$\dot{u} = Cr + \frac{D}{r} + Ir \quad (4.36)$$

where  $C$  and  $D$  are integration constants and

$$I = \frac{1}{2r^2} \int_a^r (\dot{g}_1 - 2\dot{g}_2) r dr + \int_a^r \frac{\dot{g}_1}{2r} dr \quad (4.37)$$

combining equations (4.28), (4.36) and (4.37), and after simplification we obtain

$$\dot{\sigma}_r = \frac{E}{(1+\nu)(1-2\nu)} \left( C_1 - (1-2\nu) \frac{C_2}{r^2} + I_1 + I_2 \right) \quad (4.38a)$$

$$\dot{\sigma}_\theta = \frac{E}{(1+\nu)(1-2\nu)} \left( C_1 + (1-2\nu) \frac{C_2}{r^2} - I_1 + I_2 - \frac{1-2\nu}{1-\nu} \dot{\epsilon}_\theta^c \right), \text{ where} \quad (4.38b)$$

$$I_1 = \frac{1-2\nu}{2r^2} \int_a^r (\dot{g}_1 - 2\dot{g}_2) r dr \quad \text{and} \quad I_2 = \frac{1}{2} \int_a^r \frac{\dot{g}_1}{r} dr \quad (4.39)$$

The integration constants,  $C_1$  and  $C_2$  can be calculated by applying the following boundary conditions

$$r = a \Rightarrow \dot{\sigma}_r(r) = \dot{p}_i \quad \text{and} \quad r = b \Rightarrow \dot{\sigma}_r(r) = \dot{p}_o \quad (4.40)$$

Substituting equation (4.40) into equation (4.38a) yield the following set of equations

$$C_1 = \frac{\dot{p}_o b^2 - \dot{p}_i a^2}{E(b^2 - a^2)} (1+\nu)(1-2\nu) - \frac{I_o b^2}{b^2 - a^2} \quad (4.41a)$$

$$C_2 = \frac{(\dot{p}_o - \dot{p}_i)b^2 a^2}{E(b^2 - a^2)}(1 + \nu) - \frac{I_o b^2 a^2}{(1 - \nu)(b^2 - a^2)} \quad (4.41b)$$

where  $I_o$  is defined as

$$I_o = (I_1 + I_2)_{r=b} \quad (4.42)$$

Note that, for boiler tubes assumed to be operating at steady state pressure (constant operational pressure) from the water side and fire side,  $\dot{p}_i = \dot{p}_o = 0$ , thus the integration constants given in equations (4.41) become

$$C_1 = -\frac{I_o b^2}{b^2 - a^2} \quad \text{and} \quad C_2 = -\frac{I_o b^2 a^2}{(1 - \nu)(b^2 - a^2)} \quad (4.43)$$

To obtain creep strains, two common models, i.e. time-hardening and strain-hardening are used. The time hardening hypothesis, takes the creep strain rate explicitly as a function of stress and time and implicitly as a function of temperature in the following form (see section 3.4.2)

$$\dot{\epsilon}_r^c = \frac{3}{4} \frac{K \sigma_e^{n-1}}{q} (\sigma_r - \sigma_\theta) t^{q-1} \quad (4.44a)$$

$$\dot{\epsilon}_\theta^c = \frac{3}{4} \frac{K \sigma_e^{n-1}}{q} (\sigma_\theta - \sigma_r) t^{q-1} \quad (4.44b)$$

However, the strain hardening theory assumes the creep strain rate is a function of stress, temperature and accumulated creep strain and is given in the following form

$$\dot{\epsilon}_r^c = \frac{3}{4} \frac{K \sigma_e^{n-1}}{q} (\sigma_r - \sigma_\theta) \left( \frac{\epsilon_e}{K \sigma_e^n} \right)^{\frac{q-1}{q}} \quad (4.45a)$$

$$\dot{\epsilon}_\theta^c = \frac{3}{4} \frac{K \sigma_e^{n-1}}{q} (\sigma_\theta - \sigma_r) \left( \frac{\epsilon_e}{K \sigma_e^n} \right)^{\frac{q-1}{q}} \quad (4.45b)$$

## 4.2.2 Summary of Calculation Steps

The following outlines may be followed for the calculation of stresses and strains at each instant of time step.

1. The distribution of radial, tangential and longitudinal stresses is calculated based on the basic Lamé's solution derived from equation (4.32). These are the stresses at zero time ( $t = 0$ ), when the elastic loading is complete.
2. The distributions of radial and tangential strain rates are obtained by using one or both hardening rules, equations (4.44) and/or equations (4.45).
3. The distributions of the rates of radial and tangential stresses are calculated by using the derived formulas equations (4.38).
4. If these stresses and strains are allowed to redistribute (relax) for an increment of time, select a suitable time interval  $\Delta t$ . Then the radial, tangential and longitudinal stresses at the next time step  $t + \Delta t$  are obtained by assuming

$$(\sigma_r)_{i+1} = (\sigma_r)_i + (\dot{\sigma}_r)_i \times \Delta t \quad (4.46a)$$

$$(\sigma_\theta)_{i+1} = (\sigma_\theta)_i + (\dot{\sigma}_\theta)_i \times \Delta t \quad (4.46b)$$

$$(\sigma_z)_{i+1} = \frac{1}{2} [(\sigma_r)_{i+1} + (\sigma_\theta)_{i+1}] \quad (4.46c)$$

5. Similarly, the strains at the next time is obtained by assuming

$$(\varepsilon_r)_{i+1} = (\varepsilon_r)_i + (\dot{\varepsilon}_r)_i \times \Delta t \quad (4.47a)$$

$$(\varepsilon_\theta)_{i+1} = (\varepsilon_\theta)_i + (\dot{\varepsilon}_\theta)_i \times \Delta t \quad (4.47b)$$

6. Steps 2–5 are repeated for each time step until the radial and tangential stress distributions approach a steady state condition or until the specified total time is

reached. The step at which the stress redistribution is completed is called stationary state and is defined by  $\dot{\epsilon}_r = \dot{\epsilon}_\theta = 0$ .

## **4.3 Incremental Approach ( FEM )**

### **4.3.1 Introduction**

An analysis and a numerical computer program will be developed for calculating the creep strains in an arbitrary axisymmetric tube of revolution subjected to axisymmetric loads. The method of solution is an extension of the direct stiffness method. The body is replaced by a system of discrete triangular cross section ring elements interconnected along circumferential nodal circles. The equation of equilibrium for the tube is derived from the principle of minimum potential energy. The creep behavior of the tube is obtained by the use of an incremental approach as discussed in the previous topics. The method involves starting with the elastic solution of the problem and calculating the creep strains for a small time increment. These creep strains are treated as initial strains to determine the new stress distribution at the end of the time increment. The procedure is repeated either until the final time is reached or until the stress distribution becomes constant i.e. a steady-state condition is reached. The method is quite general and is independent of the type of creep law used.

### **4.3.2 Method of Analysis**

The method of analysis used in this thesis is known as the direct stiffness or displacement method. It can best be described as a variational procedure. In classical elasticity one of the most widely used variational principles is the Theorem of Minimum Potential Energy [46]. This theorem states that of all displacement functions which satisfy the boundary

conditions, the one which satisfies the equilibrium equations makes the potential energy an absolute minimum. The direct stiffness method is a systematic procedure for the application of this theorem.

From continuum problems, the body is approximated by a set of simple sub-regions, called finite elements, which are usually taken as geometrically simple as possible. Within each element the displacements are assumed to be linear combinations of functions with undetermined coefficients, and are chosen so that continuity is preserved along the edges of adjacent elements. The assumed displacement functions for any element are related to the displacement at some particular points of the element. These points are called the nodal points of the element, and are usually taken as the corner points. The internal strain energy for each element of the body is then expressed in terms of the nodal point displacements. The potential energy for the complete body is determined by summing the strain energy for all the elements and subtracting the work done by the external loads.

Finally, minimization of the potential energy with respect to the nodal displacements yields the desired system of equations for determining the unknown nodal displacements. For programming and computational reasons, the method of constructing the governing algebraic equations is to consider each element separately. The potential energy for each element is minimized. This gives a system of equations in terms of the nodal displacements for that element and the applied forces acting on the element. The coefficient matrix for these equations is called the element stiffness matrix. The governing algebraic equations for the body are obtained by superposition of the element stiffness matrices, subject to the

condition that the displacement at any given node must be the same for all elements attached to that node. The resulting equations are modified to account for displacement boundary conditions, and are solved to yield the unknown nodal point displacements. The element strains and stresses are then calculated from the known displacements.

The inclusion of creep behavior in a finite element approach is best handled by using an incremental approach and treating the creep strains as initial strains. The solution of the problem begins by obtaining the elastic solution. Based on these stresses, the creep strains for a small time interval are computed. The results obtained are taken as initial strains for the next time interval and are included as fictitious creep forces at the nodal points in the evaluation of the nodal displacements and element stresses and strains for the next time step. The process is repeated for each increment of time. The basic assumption used in this approach is that the change in stress during any time increment is small compared to the stress at the beginning of that increment. The error introduced by this type of procedure can be made as small as one wish by reducing the time increment.

Similar procedure for solving creep problems was used by different authors. Jahed and Bidabadi [11] used incremental method to solve a problem of creep in variable material property (VMP). Gill [36] applied similar technique to discuss the stretching of a plate containing a small hole. In this part of the thesis an iterative technique will be applied to solve creep problem of boiler tubes by the FEM.

### 4.3.2.1 Derivation of Element Stiffness Relation

In applying the direct stiffness method, the first step is to choose a finite element which will be used in the representation of the body. Because of its ease to represent complex geometries, the triangular element has been the most widely used. For axisymmetric bodies, the easiest element to use is a triangular cross-sectional circular ring. Greenbaum and Rubinstein [37] used this basic element, but Jahed and Bidabadi [11] used finite number of “ring” elements in which the analysis is some how differ geometrically. They have presented a stiffness matrix for this element based on the assumption that the displacements are linear functions of the coordinates. In this thesis we will use the triangular element as shown in Fig. 4.3.

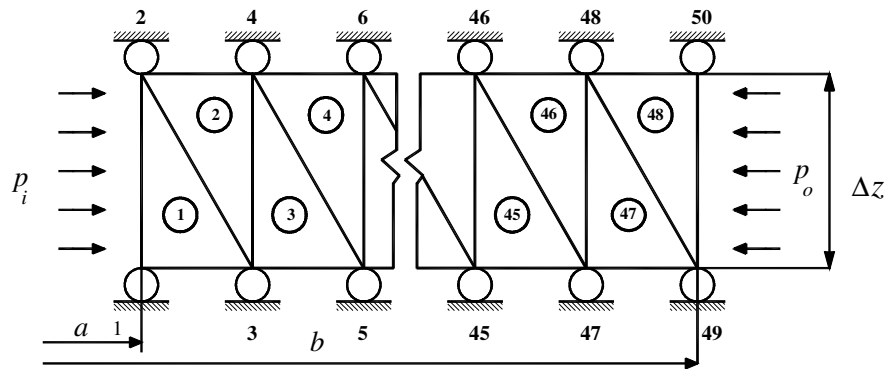


*Fig. 4.3 Infinite thick-wall tube discretized by triangular element*

The choice of the displacement functions for the element is the prime consideration in the derivation of the element stiffness matrix. The stiffness characteristics are completely specified by the choice of displacements, and therefore, the displacement functions chosen directly influence the accuracy of the solution. In general, the number of independent displacement functions to be used should equal the number of degrees of freedom of the nodal point displacements of the element. The displacement functions are chosen to

preserve continuity between elements, and the finite element solution will converge to the exact solution as the number of elements is increased. For the triangular element shown by Fig. 4.4 with nodal points at the corners, the simplest way to satisfy the above requirements is to take the displacements as linear functions of the coordinates, i.e.,

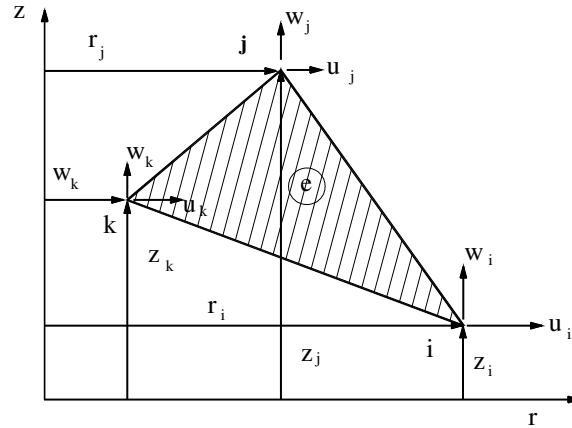


**Fig. 4.4** *Triangular element*

$$u(r, z) = a_1 + a_2 r + a_3 z \quad (4.48a)$$

$$w(r, z) = a_4 + a_5 r + a_6 z \quad (4.48b)$$

where  $a_i$  is a constant,  $i = 1, 2 \dots 6$

Another choice for the representation is to choose additional nodal points at the mid-points of the sides of the triangles. It is then possible to represent the displacements with a parabolic distribution, thus maintaining continuity along the edges of the elements since three points determine a parabolic curve. Because of the excellent results presented by Kown [39], we will use the linear distribution of displacements in the study of creep behavior of the tube. A complete derivation of the resulting stiffness matrix and load vector is given in appendix AI.

### 4.3.2.2 Multiaxial Stress-Strain-Time Relationships

In order to determine the multiaxial creep strain at any point in the body a stress-strain relation is needed. The multiaxial creep strains can be determined by following the assumptions which were discussed in section 4.1. These assumptions are satisfied by the following stress-strain relationships for a cylindrical coordinate system with rotational symmetry [41]

$$\Delta \varepsilon_r^c = \frac{\Delta \varepsilon_e^c}{2\sigma_e} (2\sigma_r - \sigma_\theta - \sigma_z) \quad (4.49a)$$

$$\Delta \varepsilon_\theta^c = \frac{\Delta \varepsilon_e^c}{2\sigma_e} (2\sigma_\theta - \sigma_r - \sigma_z) \quad (4.49b)$$

$$\Delta \varepsilon_z^c = \frac{\Delta \varepsilon_e^c}{2\sigma_e} (2\sigma_z - \sigma_r - \sigma_\theta) \quad (4.49c)$$

$$\Delta \varepsilon_{rz}^c = \frac{3\Delta \varepsilon_e^c}{2\sigma_e} \sigma_{rz} \quad (4.49d)$$

Where the effective stress,  $\sigma_e$  is defined as

$$\sigma_e = \frac{1}{\sqrt{2}} \sqrt{(\sigma_r - \sigma_\theta)^2 + (\sigma_\theta - \sigma_z)^2 + (\sigma_r - \sigma_z)^2 + 6\sigma_{rz}^2} \quad (4.50)$$

The effective incremental creep strain  $\Delta \varepsilon_e^c$  is equivalent to the uniaxial creep strain increment and is obtained from tests. In general, the effective incremental creep strain is a function of the effective stress  $\sigma_e$ , the total effective strain  $\varepsilon_e^c$ , the temperature  $T$ , the time  $t$ , and the strain history of the material, i.e.,

$$\Delta \varepsilon_e^c = f(\sigma_e, \varepsilon_e^c, T, t) \quad (4.51)$$

A number of methods have been proposed for predicting creep strains under a continuously changing stress condition, like the one proposed by Popov [40]. However, each of the methods has been shown to have shortcomings, and as yet there does not appear to be a method which is capable of predicting creep behavior in a perfectly general way. The method of solution presented here is independent of the manner in which creep strains are assumed to be accumulated, and may be used with any method. Two of the most commonly used methods of accumulating creep strains are the strain-hardening and the time-hardening laws, as discussed in section 3.4.2.

#### 4.3.2.3 Solution technique

The solution of the creep problem begins with the assumption that if there is no temperature gradient, the total change in strain during a time interval is the sum of the changes in elastic and creep strain, i.e.,

$$\{\Delta\epsilon\} = \{\Delta\epsilon^{el}\} + \{\Delta\epsilon^c\} \quad (4.52)$$

Where the superscripts *el* and *c* denote elastic and creep strain respectively. The change in the elastic strains is thus,

$$\{\Delta\epsilon^{el}\} = \{\Delta\epsilon\} - \{\Delta\epsilon^c\} \quad (4.53)$$

The incremental stresses are then related to the elastic strains by the general Hooke's law equations

$$\{\Delta\sigma\} = [D]\{\Delta\epsilon^{el}\} \quad (4.54)$$

Substituting equation (4.52) into equation (4.54) yields the relation between the incremental stress, total strain, and creep strain

$$\{\Delta\sigma\} = [D]\{\{\Delta\epsilon\} - \{\Delta\epsilon^c\}\} \quad (4.55)$$

The other field equations are obtained from the relationship between strain and deformation, the creep law of the material, and from the minimization of the potential energy of the body. These equations may be expressed as

$$\{\Delta \varepsilon\} = [B]\{\Delta u_i\} \quad (4.56a)$$

$$\{\Delta \varepsilon^c\} = \{f(\sigma_e, t, T)\} \quad (4.56b)$$

$$\{\Delta u^c\} = [K]^{-1}[F^c] \quad (4.56c)$$

Where  $\{\Delta u_i\}$  = change in nodal point displacements

$[K]$  = stiffness matrix of the body.

### 4.3.3 Solution steps

At time  $t = 0$ , the elastic stresses are determined. These stresses are assumed to remain constant during a small time increment,  $\Delta t$  and the incremental creep strains are calculated from equation (4.56b).

The creep strains are substituted into equation (4.56c) to find the total change of the nodal point displacements. These displacements are substituted into equation (4.56a) to determine the total change in strain.

Finally, the incremental stresses are obtained from equation (4.55) and are added to the previous stresses to yield the new stress distribution  $\{\sigma_{t+\Delta t}\} = \{\sigma_t\} + \{\Delta \sigma\}$ . As long as the incremental stresses,  $\{\Delta \sigma\}$ , are small compared to the previous stresses,  $\{\sigma_t\}$ , no basic assumptions are violated and the solution proceeds to the next time increment using the

same procedure. If, however, the incremental stress is not small compared to the previous stresses, the time step can be repeated with a smaller time increment.

During the initial or transient states of creep, the stresses change very rapidly so that it is necessary to choose exceptionally small time increments in this region. However, as the solution approaches a steady state condition, i.e.  $\{\Delta\sigma\} \rightarrow 0$ , it is theoretically possible to increase the time increments without violating any assumptions. Once a steady-state solution is reached, the stresses remain constant and the creep strains for future times may be obtained by extrapolation.

Where there is an inclusion of time dependent loading, it is handled by applying the load in discrete increments. The procedure is to apply an increment to the load at  $t = t_1$ , and then assume that the body creeps at this load level until the next increment of load is applied. This method is easily incorporated into the procedure described above. Now for analysis on the boiler tubes we need to take the effective creep strain, stress and time function developed for a uniaxial test performed on material of the same property, equation (3.4).

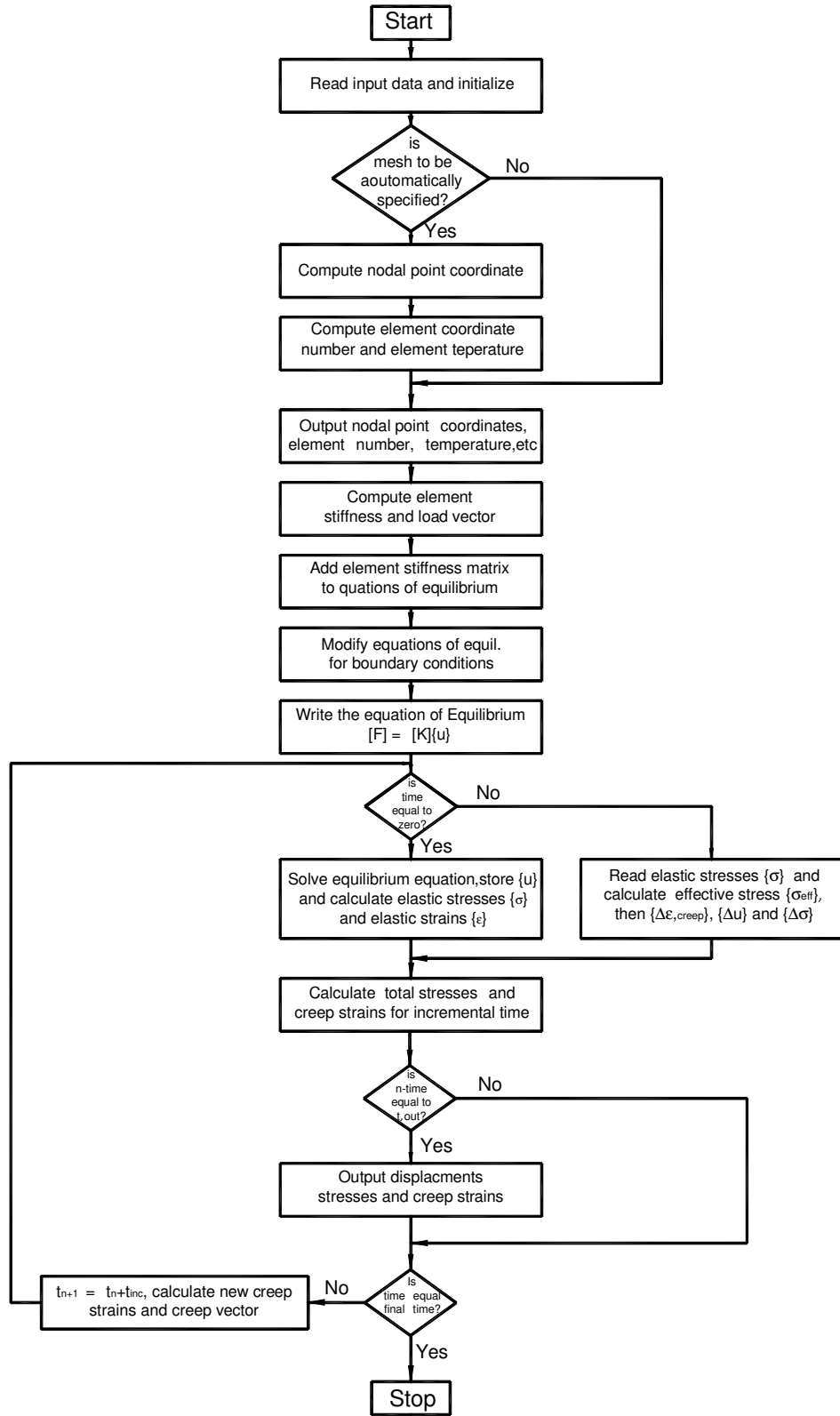


Fig. 4.5 Program flowchart

## 5 Results and Discussion

### 5.1 Input description

The input data in the derived analytical and the finite element formulations are generally categorized in to four groups. The next results were obtained based on the following data input in MATLAB program.

**General Data:** This data describes the overall problem. It gives the control parameters for the body under consideration. These are number of element, total number of nodal points and number of nodal points where boundary conditions are to be specified.

**Element Data and Nodal Point Coordinates:** This data may be input by listing the nodal point numbers, temperatures and pressure for each element, and the coordinates for each nodal point, or may be input by using the automatic mesh generator. If the automatic mesh generator is used only the inside and outside coordinates, pressures and temperatures need to be input.

**Material Data:** This data consists of Young's modulus, Poisson's ratio and coefficients of thermal expansion and the uniaxial creep law for the material under consideration.

**Boundary Conditions:** This data specifies the constraints on the nodal points i.e. the number of nodal points where displacement boundary conditions are specified.

Material	12CrMoV (DINX22CrV12I)
Uniaxial creep law	$\epsilon_e = K\sigma_e^n t^q$
	where $K = 19.64 \times 10^{-44}$ , $n = 4.4$ and $q = 1$
Inside diameter	$2a = 100mm$
Outside diameter	$2b = 150mm$
Operation temperature	$T = 500^\circ C$
Operation pressure	$P = 100MPa$
Poisson's ratio	$\nu = 0.33$
Young's modulus	$E = 207GPa$
Thermal expansion	$\alpha = 6.2 \times 10^{-6}$

## 5.2 Output Data and Discussion of Results

The output data consists of the following three groups of results.

**Problem Data:** This is the listing of all the input data for the problem under consideration.

It includes the element, nodal point and boundary condition data. This data is displayed as part of the output.

**Nodal Point Displacements:** A complete listing of all nodal point displacement at the current time (time of observation) is displayed in the output.

**Element Stresses and Creep Strains:** The stresses and creep strains for each of the discrete element of the tube are displayed in the output. Fig. 5.1 shows the elastic stress

distributions, and we can see that the FE solution is in agreement with the analytical solution. In the cases when there is small temperature gradient between the inner wall and the external wall of the tube differential stress will be developed. If we assume a temperature difference of  $10^{\circ}C$  between the inner and external wall, the resulting stress distribution due to thermal loading is shown by Fig. 5.2. Fig. 5.3 shows the dependence of the effective strain on time. From the diagram we can clearly see when the effective strain reaches the limiting value. In most tube materials the recommend strain in 10,000 hour is about 1% . The total effective strain distribution is more clearly legible if we plot them for some selected time values as shown by Fig. 5.4. Fig. 5.5 shows the contribution of each strain component at the selected time of 10,000 hours. Finally the comparison of the elastic stress and the steady state stress distribution, which includes the effect of creep and temperature gradient, is shown in Fig. 5.6.

As time passed while the boiler tube is under operation the total strain is getting higher and will reach the limiting point. This is due to the gradual increase of creep strain, since the elastic and the thermal strains remain constant as long as no temperature and pressure variation respectively. In Fig. 5.5 we can see that the creep strain take the larger contribution to the total strain. While the tube is stretching due to the increase in total strain the stress is also relaxing. The elastic stress distributions are changing and will have the arrangement as shown by Fig. 5.6.

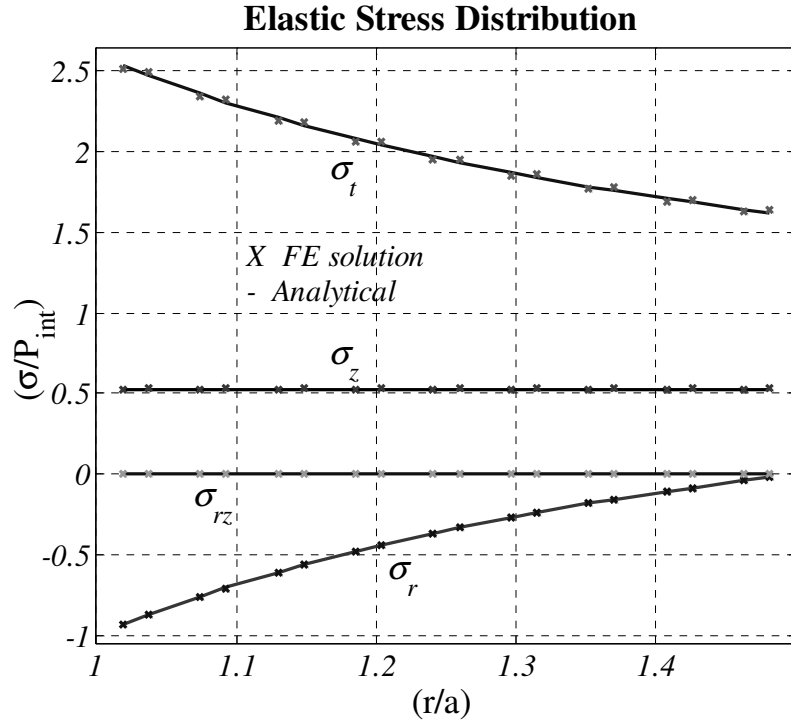


**Fig. 5. 1** Elastic stress distribution

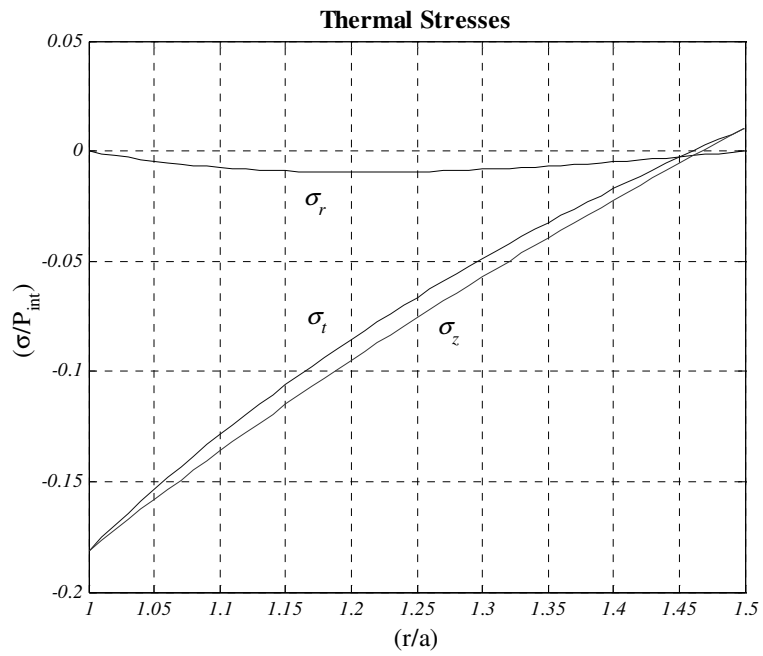


**Fig. 5. 2** Stress distribution due to temperature gradient

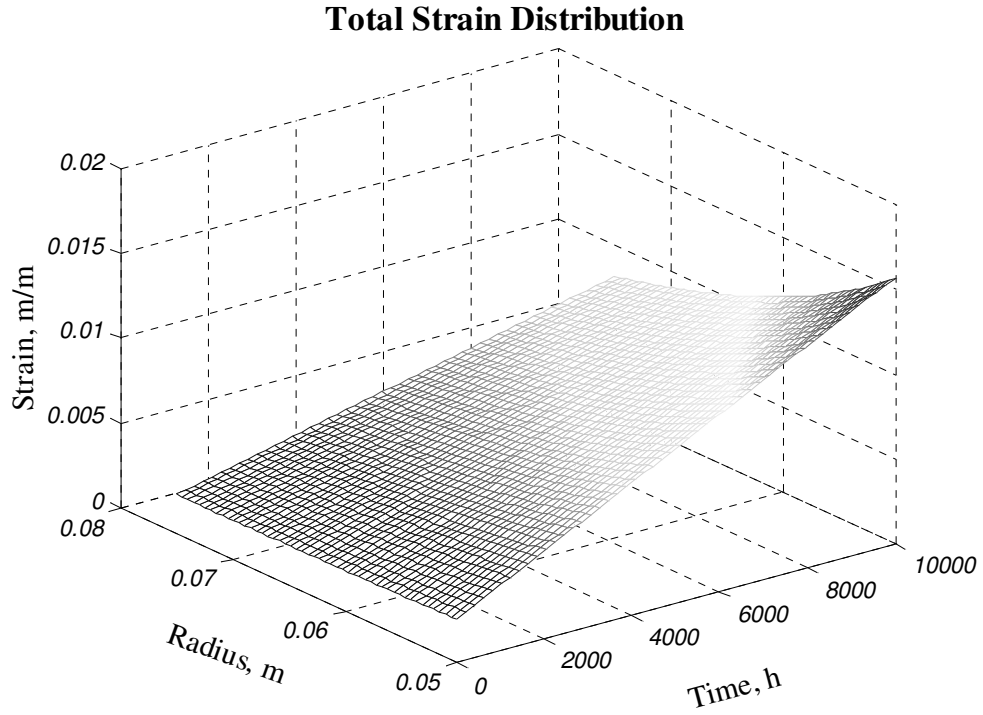


*Fig. 5. 3 Effective total strain distribution*

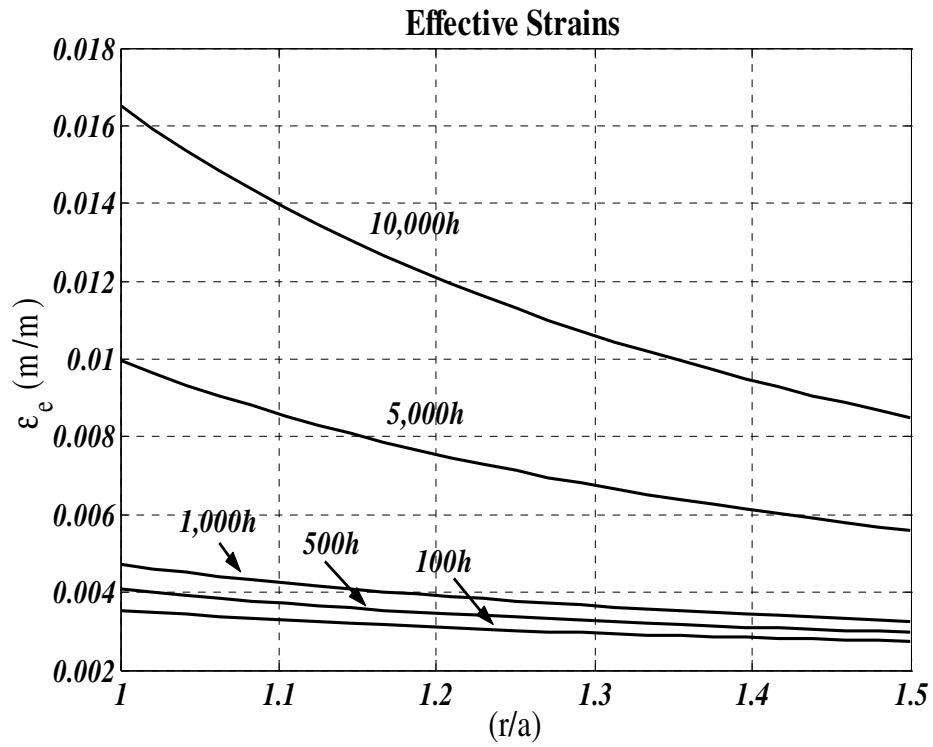


*Fig. 5. 4 Effective total strain distribution (2D)*

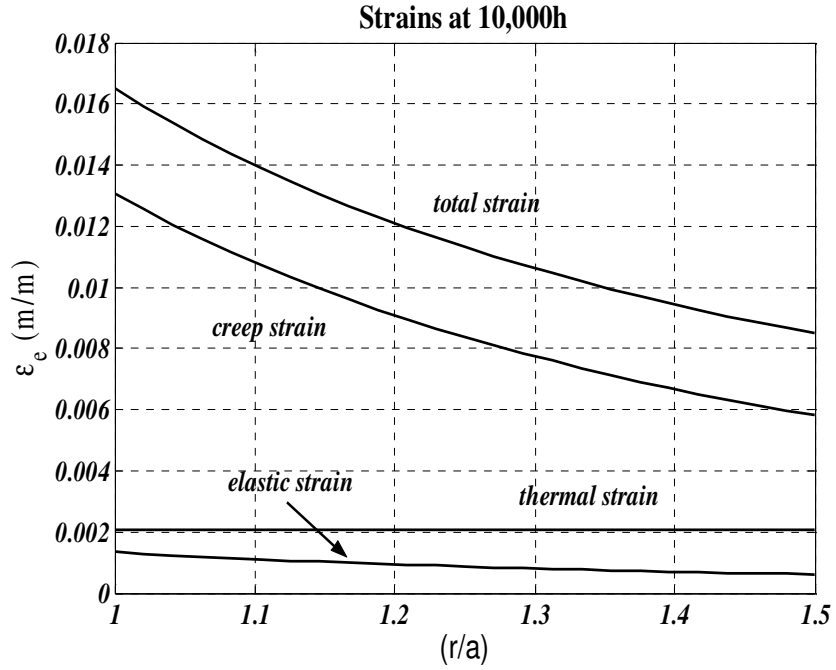


Fig. 5. 5 Strain distribution at 10,000 hour

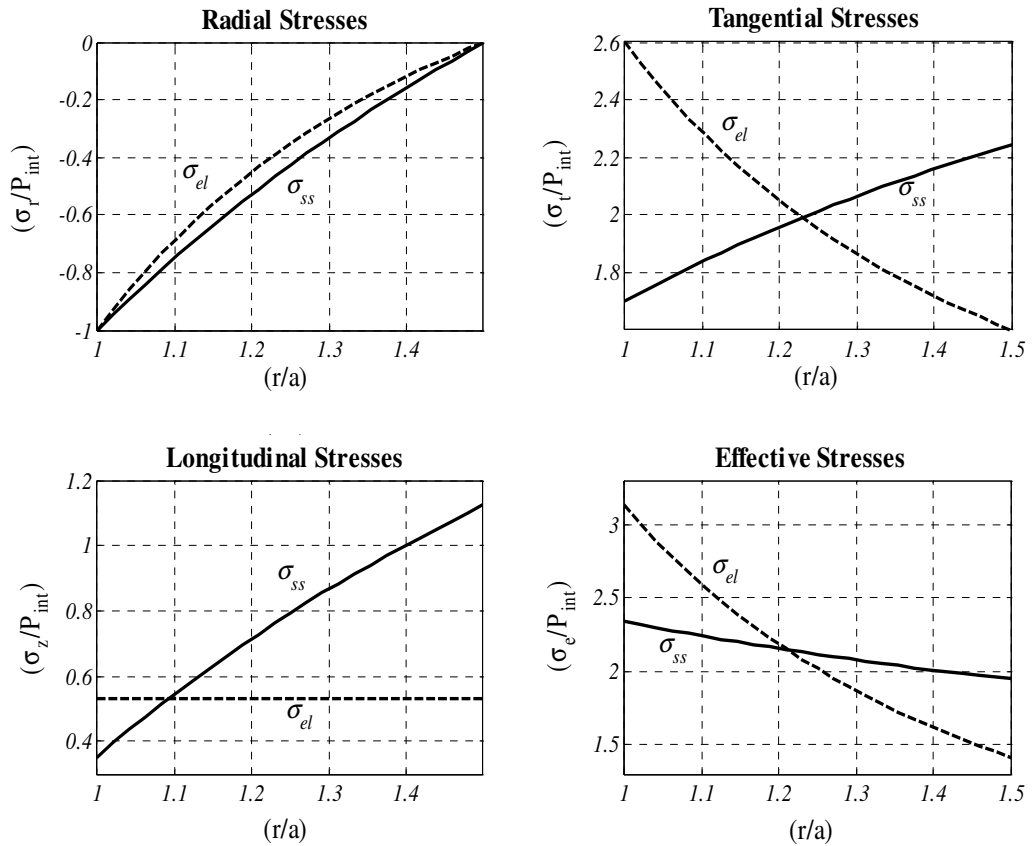


Fig. 5. 6 Elastic and relaxed stresses distribution

## **6 Conclusion and Recommendation**

### **6.1 Conclusion**

In this thesis, three distinct methods have been presented for obtaining the creep behavior of an axsymmetric boiler tubes which are subjected to an axsymmetric pressure and temperature loading. The first is the analytical solution (closed form solution) which is simple and can be used by designers as preliminary estimation of creep stresses and creep strains distribution. The solution for the stress and creep strain distributions are easily obtained when the tube attains steady state conditions. In the analytical theory, the initial elastic deformation and the transient creep deformation are neglected, since they are normally small as compared to the secondary creep deformation.

The formulation of creep equation in this analytical approach is possible only for homogeneous, isotropic and geometrically defined shape of materials, like the boiler tube we considered. Cases of temperature gradient along the tube wall can be included in the formulation with slight modification of the derived equation as discussed in section 4.1. But in the case when material nonlinearity and stresses concentration factors like cracks and scars exist, the problem becomes more complicated. In this case the analytical method is limited to handle the problem and therefore, development of more advanced method is important.

The second method developed in this thesis was the analytical incremental method. Like the closed form solution, the method may be used only for basic geometrical shapes like cylindrical tubes, but unlike the first method, material nonlinearity can be handled in this second method. In the analytical incremental method the basic solution of a uniform homogeneous axisymmetric member is used to generate solution for non uniform and/or inhomogeneous tubes. The method is capable in determining the primary and secondary creeps in inhomogeneous tubes. For creep analysis of an inhomogeneous axisymmetric body, the method already derived can be modified by discretizing the tube into a finite number of concentric tubes with constant material properties. These concentric tubes are assumed to be subjected to a stress rate at the inner and outer radius, as illustrated by equation (4.38) for each discretized tubes the governing equation (4.33) will be solved to determine the creep behavior.

Finally, we proposed that comprehensive methods should be available for handling creep problems without some of the limitations mentioned above. The third method, the incremental method by finite element formulations can be one of these methods. In the FE method material nonlinearity, loading nonlinearity and geometric complexities can be handled as long as the finite element mesh can be generated successfully. Since the method makes possible the study of creep behavior of complex geometries, the creep analysis of cracked tubes, corroded or eroded and/or pitted boiler tubes can be analyzed by developing the finite element formulation of the problems. The first or the second methods were enough for creep analysis of normally operating non damaged boiler tubes. But since practical boiler tubes are operating with surface cracked and/or pitted, we propose FE method should be used for precise creep analysis.

## **6.2 Recommendation for Future Research**

During the course of this investigation, three major areas were encountered for which further work is needed. The first area is the creep behavior and life analysis of cracked boiler tubes. In our analysis we considered very simplified assumptions that the surface of the tube is clean and no crack initiated or pitting formed on the surface. If we consider actual boiler tubes, soot deposit, scale formation and cracks are commonly encountered on the surface of tubes. Transversal and longitudinal through crack or cracks to some depth are practically possible. Thus, the analysis of cracked tubes should be the next area of investigation.

The second major area of further study may be the cases of surface pitted and corroded boiler tubes. While operation, boiler tubes are exposed to abrasion and corrosion by the particles in the flue gas and steam and/or water respectively. Therefore, somehow similar to the crack problems, the already developed finite element method may be further developed to study the creep behavior of such eroded or corroded tubes.

Another major area of further study is the analysis of swelled tubes and the case of large plastic deformations. Deposition of soot and scale on tube surface and shortage of feed water to the tube are typical factors which lead to localized overheating of tube material. Localized overheating or overall overheating will subject the tube to a net section collapse and plastic flow. Therefore, unlike the assumptions of small deformation analysis large deformations and material nonlinearity should be investigated during the plastic flow

process. To our knowledge on these areas full and complete studies were not undertaken, thus we think these will be an interesting area of research.

## References

---

- [1] Koh S. K., “Fatigue damage evaluation of a high pressure tube steel using cyclic strain energy density”, *Int. J. of Pressure Vessels and Piping*, 79 (2002) 791-8.
- [2] Goel R. P., “On the Creep Rupture of a Tube and a Sphere”, *Journal of Applied Mechanics*, (Sep 1975) 625-8.
- [3] Chen H. F., Engelhardt M. J. and Ponter A. R., “Linear matching method for creep rupture assessment”, *Int. J. Pres. Ves. & Piping*, 80 (2003) 213-220.
- [4] Yue, Z. F., Lu Z.Z. and Wang X.M., “A numerical study of damage development and creep life in circular notched specimens during creep”, *Science Reviews* 2002.
- [5] Altenbach H., “A Nonclassical Model for Creep-Damage Processes”, *Advanced Study Center Co. Ltd*, 2001.
- [6] Kwon O. et. al., “Effects of residual stress in creep crack growth analysis of cold bent tubes under internal pressure”, *Int. J. Pres. Ves. & Piping*, 78 (2001) 343-350.
- [7] Wasmer K. et al, “Creep crack initiation and growth in thick section steel pipes under internal pressure”, *Int. J. Pres. Ves. & Piping*, 80 (2003) 489-498.
- [8] Singh P.K. et al, “Crack initiation and growth behavior of circumferentially cracked pipes under cyclic and monotonic loading”, *Int. J. P. Ves. & Piping* 80 (2003) 629-640.
- [9] Nikbin K.M. et al, ”Probabilistic analysis of creep crack initiation and growth in pipe components”, *Int. J. of Pressure Vessels and Piping*, 60 (2003) 585-595.
- [10] Sanal Z., “Nonlinear analysis of pressure vessels: some examples”, *Int. J. of Pressure Vessels and Piping*, 77 (2000) 705-70

- [11] Jahed H. and Bidabadi J., “An Axisymmetric Method of Creep Analysis for Primary and Secondary Creep”, *Int. J. Pres. Ves. & Piping*, 80(2003) pp. 597-606.
- [12] Zarrabi K. and Modarres-Motlagh A., “An approximate and computationally efficient algorithm for computing reference stress for creep life assessment”, *Int. J. Pres. Ves. & Piping*, 75 (1998) 459-465.
- [13] Zarrabi K. and Zhang H., “Primary Stress in Scarred Boiler Tubes”, *International Journal of Pressure Vessels and Piping*, 65 (1995) 157-161.
- [14] Zarrabi K. and Hosseini-Toudeshky H., “Creep life assessments of Defect-Free Components under Uniform Load and Temperature”, *Int. J. Pres. Ves. & Piping*, 62 (1995) 195-200.
- [15] Zarrabi K. et al, “Estimation of metal temperature variations for scarred boiler tubes”, *Int. J. Pres. Ves. & Piping*, 69 (1996) 239-246.
- [16] Zarrabi K., “Estimation of Boiler Tube Life in Presence of Corrosion and Erosion Processes”, *Int. J. of Pres. Ves. & Piping*, 53 (1993)35 1-358.
- [17] Meggyes A. and József Új, “Stress Computation Algorithm for Temperature Dependant Non-Linear Kinematical Hardening Model”, *Periodical Polytechnic Ser. Mech. Eng. Vol. 44 No 1, Pp 105-114 (2000)*
- [18] Fett T., “Temperature Distributions and Thermal Stresses in Asymmetrically Heat Radiated Tubes”, *Trans. of the ASME, J. of A. Mech.*, 1986 Vol. 53 pp 116-120.
- [19] Wilson J.F. and Orgill G., “Linear Analysis of Uniformly Stressed, Orthotropic Cylindrical shells”, *Journal of applied mechanics June 1986, Vol. 53.*
- [20] Ponter A.R., “Deformation Bounds for the Bailey-Orowan Theory of Creep”, *J. of applied mechanics September 1975.*

- [21] Cocks C. F. and Leckie F. A., “Deformation Bounds for Cyclically Loaded Shell Structures Operating Under Creep Conditions”, *Transaction of the ASME, Journal of Applied Mechanics*, 1975 Vol. 55 pp 509-516
- [22] Cocks C. F. and Leckie F. A., “Creep Rupture of Shell Structures Subjected to Cyclic Loading”, *Transaction of the ASME, Journal of Applied Mechanics*, 1988 Vol. 55 pp 294-298.
- [23] Ling X. et al, “Damage Mechanics Considerations for Life Extension of High-Temperature Components”, *ASME, J. of Pressure Vessel Technology*, 2000 Vol.122 pp.174-179.
- [24] Zervos A. et al, “Modeling of Localization and Scale Effect in Thick-Walled Cylinders with Gradient Elastoplasticity”, *Int. J. Solids Structures*.
- [25] Hyer M. W. and Cooper D. E., “Stresses and Deformations in Composite Tubes Due to a Circumferential Temperature Gradient”, *Transaction of the ASME Journal of Applied Mechanics*, 1986 Vol. 53 pp.757-764.
- [26] Orgill G. and Wilson J.F., “Finite Deformations of Nonlinear Orthotropic cylindrical Shells”, *Journal of applied mechanics June 1986, Vol.53*.
- [27] Manson S.S., *Thermal stress and Low-cycle Fatigue*, McGraw-Hill book, 1966.
- [28] Harvey J. F., *Theory and design of pressure vessels*, Chapman and hall, 1991.
- [29] Hetnarski R. B., *Thermal Stresses I, Mechanical and Mathematical Methods*, Rochester Institute of Technology Rochester, New York, 1996.
- [30] Dehnel P. D., *Fundamentals of Boiler House Technique*, Hutchinson & Co. Publisher Ltd, 1959.
- [31] Lemaitre J. and Chaboche J.L., *Mechanics of Solid Materials*, Cambridge University Press, 1985.

- [32] Farr J. R. and Jawad M. H., *Guidebook for the Design of ASME Section VIII Pressure Vessels*, ASME press, 1998.
- [33] Ogata T. and Yaguchi M., “Study on Creep-Fatigue Damage Evaluation for Boiler Weldment Parts”, *ASME, J. of Pressure Vessel Tech.*, 2001 vol. 78 pp 105-111.
- [34] Timoshenko S., *Strength of Materials, Part II Advanced Theories and Problems*, Van Nostrand Reinhold Company, 1958.
- [35] Brandes E.A. and Brook G.B., *Smithells Metals Reference Book, Seventh edit.*
- [36] Gill S.S., *The Stress Analysis of Pressure Vessels and Pressure Vessel Components*, Pergamon Press, 1970.
- [37] Greenbaum G. A. and Rubinstein M. F., “Creep Analysis of Axisymmetric Bodies Using Finite Elements”, *Nuclear Engineering and Design*, 1968.
- [38] Coffin L. F. et al, “Primary Creep in the Design of Internal-Pressure Vessels”, *Transaction of the ASME Journal of Applied Mechanics*, 1949.
- [39] Kwon Y. W. and Bang H., *The Finite Element Method Using MATLAB*, 2ed, CRS press LLC, 2000.
- [40] Popov E. P., “Correlation of Tension Creep Tests with Relaxation Tests”, *Transaction of the ASME Journal of Applied Mechanics*, 1947.
- [41] Bailey R. W., “Design Aspect of Creep”, *Transaction of the ASME Journal of Applied Mechanics, Vol. 1.*
- [42] Guan Z. W. and Boot J. C., ”Creep Analysis of Polymeric Pipes under Internal Pressure”, *Polymer Engineering and Science, June 2001, vol. 41, No. 6.*
- [43] Pao Y. and Marin J., ”An Analytical Theory of the Creep Deformation of Materials”, *Trans. of the ASME J. of Applied Mech., June 1953.*

- [44] Kim Y. J. et al, "Estimation of creep fracture mechanics parameters for through-thickness cracked cylinders and finite element validation", *Blackwell publishing Ltd. Fatigue Frac. Engng. Mater struct.* 26, 229-244.
- [45] Kim Y. J. et al, "Reference Stress Based J and COD Estimations for LBB Analysis and Comparison with GE/EPRI Method", *SAFE Research Center, Sungkyunkwan University, Suwon , Korea.*
- [46] Zienkiewicz O. C., *The Finite Element Method*, 3ed. McGRAW-HILL Book Company Ltd., 1977.
- [47] Port R. D. and Herro H. M., *The NALCO Guide to Boiler Failure Analysis*, Nalco Chemical Company, McGraw-Hill, Inc, 1991.
- [48] Fanpel J. H. and Fisher F. E., *Engineering design, a synthesis of stress analysis and materials engineering*, 2<sup>nd</sup> ed, John Wiley and sons, 1981

### Derivation of Element Stiffness Relations

Consider the triangular element as shown in Fig. AI. 1. The coordinate system for this element is taken as a cylindrical system with the z-axis coincident with the axis of symmetry. The displacements of the element are assumed to be of the following form:

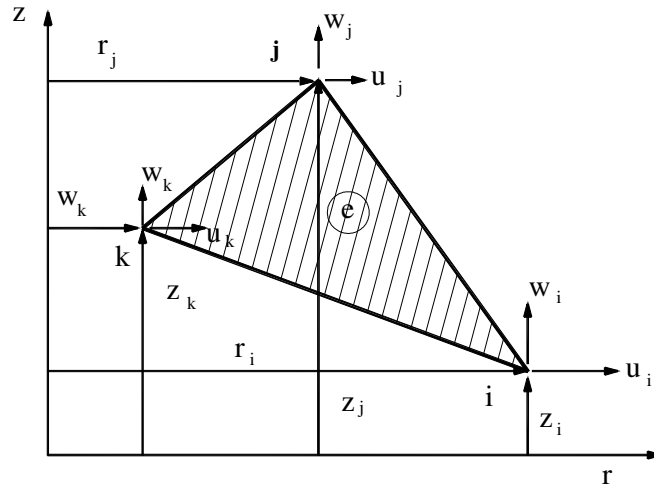


Fig. AI.1 Triangular element

$$\begin{Bmatrix} u(r, z) \\ w(r, z) \end{Bmatrix} = \begin{bmatrix} 1 & r & z & 0 & 0 & 0 \\ 0 & 0 & 0 & 1 & r & z \end{bmatrix} \begin{Bmatrix} a_1 \\ a_2 \\ a_3 \\ a_4 \\ a_5 \\ a_6 \end{Bmatrix} \text{ or} \tag{AI.1}$$

$$\{u\} = [\Phi] \{a\} \tag{AI.2}$$

By evaluating equation (AI.1) at each of the three vertices of the triangle, the following relation is obtained

$$\begin{Bmatrix} u_i \\ w_i \\ u_j \\ w_j \\ u_k \\ w_k \end{Bmatrix} = \begin{bmatrix} 1 & r_i & z_i & 0 & 0 & 0 \\ 0 & 0 & 0 & 1 & r_i & z_i \\ 1 & r_j & z_j & 0 & 0 & 0 \\ 0 & 0 & 0 & 1 & r_j & z_j \\ 1 & r_k & z_k & 0 & 0 & 0 \\ 0 & 0 & 0 & 1 & r_k & z_k \end{bmatrix} \begin{Bmatrix} a_1 \\ a_2 \\ a_3 \\ a_4 \\ a_5 \\ a_6 \end{Bmatrix} \quad \text{or} \quad (\text{AI.3})$$

$$\{u_i\} = [\Gamma] \{a\} \quad (\text{AI.4})$$

The generalized displacement vector  $\{a\}$  is now expressed in terms of the nodal point displacement by inverting equation (AI.4), i.e.

$$\{a\} = [\Gamma]^{-1} \{u_i\} = [H] \{u_i\} \quad (\text{AI.5})$$

where

$$[H] = [\Gamma]^{-1} = \frac{1}{2A} \begin{bmatrix} r_j z_k - r_k z_j & 0 & r_k z_i - r_i z_k & 0 & r_i z_j - r_j z_i & 0 \\ z_j - z_k & 0 & z_k - z_i & 0 & z_i - z_j & 0 \\ r_k - r_j & 0 & r_i - r_k & 0 & r_j - r_i & 0 \\ 0 & r_j z_k - r_k z_j & 0 & r_k z_i - r_i z_k & 0 & r_i z_j - r_j z_i \\ 0 & z_j - z_k & 0 & z_k - z_i & 0 & z_i - z_j \\ 0 & r_k - r_j & 0 & r_i - r_k & 0 & r_j - r_i \end{bmatrix} \quad (\text{AI.6})$$

$$\text{where } 2A = r_i(z_j - z_k) + r_j(z_k - z_i) + r_k(z_i - z_j)$$

The strain displacement relation in cylindrical coordinates are given by

$$\varepsilon_r = \frac{\partial u}{\partial r}, \quad \varepsilon_\theta = \frac{u}{r}, \quad \varepsilon_z = \frac{\partial w}{\partial z}, \quad \gamma_{rz} = \left( \frac{\partial u}{\partial z} + \frac{\partial w}{\partial r} \right) \quad (\text{AI.7})$$

Substituting equation (AI.1) into (AI.7) yields:

$$\begin{Bmatrix} \varepsilon_r \\ \varepsilon_z \\ \varepsilon_\theta \\ \varepsilon_{rz} \end{Bmatrix} = \begin{bmatrix} 0 & 1 & 0 & 0 & 0 & 0 \\ 0 & 0 & 0 & 0 & 0 & 1 \\ \frac{1}{r} & 1 & \frac{z}{r} & 0 & 0 & 0 \\ 0 & 0 & 1 & 0 & 1 & 0 \end{bmatrix} \begin{Bmatrix} a_1 \\ a_2 \\ a_3 \\ a_4 \\ a_5 \\ a_6 \end{Bmatrix} \quad \text{or} \quad (\text{AI.8})$$

$$\{\varepsilon\} = [N] \{a\} \quad (\text{AI.9})$$

For the solution of the creep problem the strain  $\{\epsilon\}$  is assumed to be composed of the elastic strain, thermal strain, and creep strain

$$\{\epsilon\} = \{\epsilon^{el}\} + \{\epsilon^c\} + \{\alpha\Delta T\} \quad (\text{AI.10})$$

Solving equation (AI.10) for the elastic strain gives

$$\{\epsilon^{el}\} = \{\epsilon\} - \{\epsilon^c\} - \{\alpha\Delta T\} \quad (\text{AI.11})$$

The stress strain relations for an elastic isotropic material are

$$\begin{Bmatrix} \sigma_r \\ \sigma_z \\ \sigma_\theta \\ \sigma_{rz} \end{Bmatrix} = \frac{E}{(1+\nu)(1-2\nu)} \begin{Bmatrix} 1-\nu & \nu & \nu & 0 \\ \nu & 1-\nu & \nu & 0 \\ \nu & \nu & 1-\nu & 0 \\ 0 & 0 & 0 & \frac{1-2\nu}{2} \end{Bmatrix} \begin{Bmatrix} \epsilon_r^{el} \\ \epsilon_z^{el} \\ \epsilon_\theta^{el} \\ \epsilon_{rz}^{el} \end{Bmatrix} \quad (\text{AI.12})$$

Substituting equation (AI.11) into (AI.12) and using the relation that the creep strains are incompressible yields

$$\begin{Bmatrix} \sigma_r \\ \sigma_z \\ \sigma_\theta \\ \sigma_{rz} \end{Bmatrix} = \frac{E}{(1+\nu)(1-2\nu)} \begin{Bmatrix} 1-\nu & \nu & \nu & 0 \\ \nu & 1-\nu & \nu & 0 \\ \nu & \nu & 1-\nu & 0 \\ 0 & 0 & 0 & \frac{1-2\nu}{2} \end{Bmatrix} \begin{Bmatrix} \epsilon_r \\ \epsilon_z \\ \epsilon_\theta \\ \epsilon_{rz} \end{Bmatrix} - \frac{E}{1+\nu} \begin{Bmatrix} \epsilon_r^c \\ \epsilon_z^c \\ \epsilon_\theta^c \\ \epsilon_{rz}^c \end{Bmatrix} - \frac{E\alpha\Delta T}{1-2\nu} \begin{Bmatrix} 1 \\ 1 \\ 1 \\ 0 \end{Bmatrix} \quad (\text{AI.13})$$

or symbolically

$$\{\sigma\} = [D] \{\epsilon\} - \frac{E}{1+\nu} \{\epsilon^c\} - \frac{E}{1-2\nu} \{\epsilon^{th}\} \quad (\text{AI.14})$$

The stiffness matrix for the element may now be determined from the Theorem of Minimum Potential Energy. The principle states “*of all kinematically admissible configurations, the deformation producing the minimum total potential energy is the stable equilibrium condition*”. Therefore:

$$\delta U = 0 \quad (\text{AI.15})$$

The potential energy for the element is:

$$U = \frac{1}{2} \int_V \{\boldsymbol{\varepsilon}^T\} [D] \{\boldsymbol{\varepsilon}\} dV - \frac{E}{1+\nu} \int_V \{\boldsymbol{\varepsilon}^T\} \{\boldsymbol{\varepsilon}^c\} dV - \frac{E}{1-2\nu} \int_V \{\boldsymbol{\varepsilon}^T\} \{\boldsymbol{\varepsilon}^{th}\} dV - \int_{A_p} \{\boldsymbol{u}^T\} \{P\} dA_p \quad (\text{AI.16})$$

Where  $V$  = volume of the element

$A_p$  = area over which the surface forces  $P$  are specified.

Substituting equations (AI.12), (AI.9) and (AI.16) into (AI.15) gives

$$\delta U = \delta \left\{ \frac{1}{2} \int_V \{\boldsymbol{\varepsilon}^T\} [D] \{\boldsymbol{\varepsilon}\} dV - 2G \int_V \{\boldsymbol{\varepsilon}^T\} \{\boldsymbol{\varepsilon}^c\} dV - \frac{E}{1-2\nu} \int_V \{\boldsymbol{\varepsilon}^T\} \{\boldsymbol{\varepsilon}^{th}\} dV - \int_{A_p} \{\boldsymbol{\Phi}^T\} \{P\} dA_p \right\} = 0 \quad (\text{AI.17})$$

Taking variations of (AI.17) with respect to the generalized displacements  $\{a\}$  yields the following system of equations:

$$[k] \{a\} = \{f\} \quad (\text{AI.18})$$

where

$$\{k\} = \int_V [N^T] [D] [N] dV$$

$$\{F\} = 2G \int_V [N^T] \{\boldsymbol{\varepsilon}^c\} dV + \frac{E}{1-2\nu} \int_V [N^T] \{\boldsymbol{\varepsilon}^{th}\} dV + \int_{A_p} [\boldsymbol{\Phi}^T] \{P\} dA_p = \{F^C\} + \{F^{th}\} + \{F^P\}$$

Thus far the stiffness matrix and load vector which have been presented are with respect to the generalized displacements  $\{a\}$ , equation (AI.18). However, it is much more convenient for combining stiffness matrices of adjacent elements to work with the nodal displacements. Since the nodal displacements are related to the generalized displacements through equation (AI.5). Substituting into (AI.18) and premultiplying by  $[B^T]$  yields the desired relationship:

$$[B^T] [k] [B] \{u_i\} = [B^T] \{f\} \quad \text{or} \quad (\text{AI.19})$$

$$[K]\{u_i\} = \{F_i\} \quad (\text{AI.20})$$

where

$$[K] = [B]^T [k] [B] \quad \text{and} \quad \{F_i\} = [B]^T \{f\}$$

Once the element stiffness matrix and load vector have been evaluated, they are assembled into a set of  $2 \times nel$  equations of equilibrium for the body ( $nel$  = number of nodal points). Equilibrium requires that all element forces at node  $i$  be in equilibrium with the external forces at that node. This is accomplished by adding the equations of all elements associated with the forces at that point, i.e.

$$\{P\} = \sum_{j=1}^{nel} \{F_i\}_j \quad (\text{AI.21})$$

Substituting Equation (AI.20) into (AI.21), and specifying that the displacement at any given node be the same for all elements attached to that node (i.e., compatibility), gives:

$$\{P\} = \sum_{j=1}^{nel} \{F_i\}_{nel} = \sum_{j=1}^{nel} [K]_j \{u_i\} \quad \text{or} \quad (\text{AI.22})$$

$$[K] \{u_i\} = \{P\} \quad (\text{AI.23})$$

where  $[K]$  is a  $2 \times nel$  by  $2 \times nel$  symmetric matrix. After the stiffness matrix for the body is assembled, displacement boundary conditions are specified and the matrix is constrained. The constrained equations of equilibrium are then solved by the method discussed in section 4.3.2.3.